



THE UNIVERSITY *of* EDINBURGH
School of Biological Sciences

Disentangling patterns of gene expression in high grade serous ovarian cancer

Student Exam Number: **B156476**

In partial fulfilment of the requirement for the Degree of Master of Science in Systems and Synthetic Biology at the University of Edinburgh, 2019 / 2020

Dissertation Supervisor: Dr. Ailith Ewing

Contents

1	Introduction	3
1.1	Matrix factorization	3
1.1.1	Determining the optimum number of factors	6
1.2	Gene expression in HGSOC	6
1.3	Research questions	8
2	Methodology	9
2.1	Outline	9
2.1.1	Datasets	9
2.1.2	Method outline	9
2.1.3	Tools	11
2.2	Data normalization and quality control	11
2.3	Gene set intersection	12
2.4	Matrix factorization computation	12
2.5	Metagene selection by cluster coherence	13
2.6	Gene enrichment analysis	14
2.7	Transfer of learned metagenes to novel a dataset	16
2.8	Reconciling computed metasamples and metadata	18
2.9	Survival analysis	18
2.10	Metasample heatmap analysis	19
2.11	Codebase	19
3	Results	19

3.1	Cluster coherence analysis results	19
3.2	Gene Enrichment (against GO) Results	23
3.3	Survival analysis results	24
3.4	Metasample heatmap clustering results	24
4	Discussion	36
4.1	Research questions revisited	38
4.2	Further work	38
5	Conclusions	39
6	Appendices	43
6.1	Additional figures and plots	43
6.2	Gene enrichment raw results	43
6.3	Software libraries and versions	43

1 Introduction

High grade serous ovarian cancer (HGSOC) effects the epithelium of the ovaries and fallopian tubes. “Serous” refers to the epithelial membrane which secretes serous fluid (serum). It is the 7th most common cancer in women worldwide . Epithelial ovarian cancers are classified into two broad subtypes: Type I are low grade with generally good prognosis; type II are more aggressive and typically carry P53 mutations with defects in mechanisms of DNA repair. Type II is more-or-less synonymous with HGSOC. [1].

This work is concerned with analysing the patterns gene expression in HGSOC by dimensionality reduction techniques of matrix factorization, and relating these patterns to clinical and genomic features.

1.1 Matrix factorization

A good introduction to field is ref [2], in which matrix factorization (MF) methods are discussed as a means of extraction the low dimensional structure from a high dimensional “-omics” datasets, with gene expression analysis being the prime example.

The three matrix factorization methods of interest to this work are listed below. All are forms of dimensionality reduction, but have differing criteria they aim to optimise. The number of target dimensions (or components, factors, metagenes) is referred to as the rank, k .

Non-negative matrix factorization (NMF). As the name implies, this is only applicable to matrices with +ve or zero elements, and finds components which are themselves +ve or zero. This property make the resulting factorization more interpretable since the components are strictly additive. It also allows for input samples to be directly assigned to one of k clusters. A good description of NMF and its applications in bioinformatics can be found in [3].

Independent component analysis (ICA). The goal of ICA is to represent the given matrix with components which are statistically independent of each other. It was originally proposed to solve the blind source separation problems [4]. If the input matrix of samples were drawn from a multivariate Gaussian distribution, then the result would be no different to that of PCA. Where the data is non-Gaussian however, ICA results in components which separate out independent sources of variation. See [5] for a full explanation, from which figure 1 is taken.

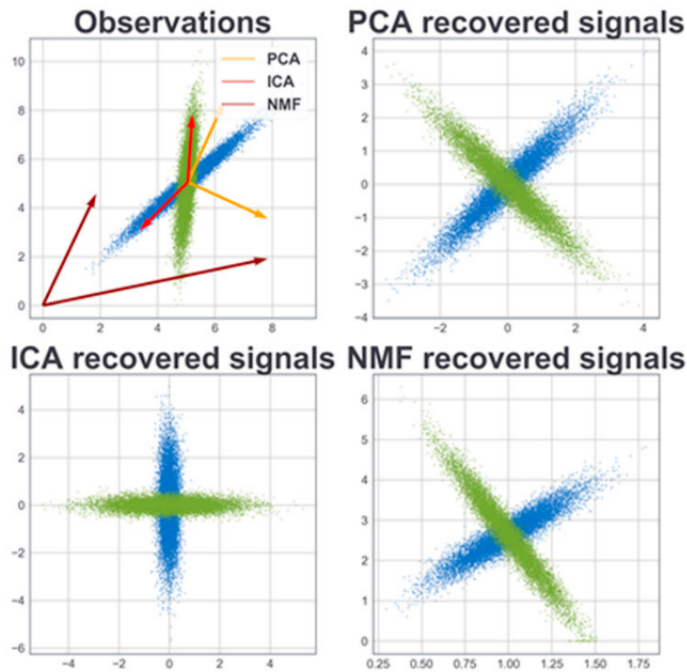


Figure 1: Illustrating the differing results of component extraction by PCA, ICA and NMF. From [5]

Principal component analysis (PCA). PCA is a well known technique for dimensionality reduction, based on eigenvalue decomposition. It is the ideal, efficient solution for multivariate Gaussian distributed data.

The contrasting results of the three methods is illustrated in figure 1.

Conventionally, transcriptomics expression arrays are oriented with genes (or transcripts) as rows, and samples (e.g. patients) in columns. A typical expression array might have in the order of tens of thousands of rows and hundreds of columns. MF methods reduces this large $M \times N$ (genes \times samples) matrix into two two smaller matrices. In the general terminology of Stein-O'Brien *et al* these are the $M \times K$ *pattern matrix* and the $K \times N$ *amplitude matrix*. K is typically small of the order 10, and refers to the number of extracted *factors* (or components). Since we are focussing on transcriptomics, rather than pattern and amplitude we will use the terms *metagenes* and *metasamples* respectively, which are in common useage. The symbol conventions for these matrices varies depending whether NMF, ICA or PCA is being discussed. NMF generally uses W and H respectively while ICA generally uses S and A . PCA tends to be differently formulated, but W and T sometimes used. The original matrix to be factorized is variously named X or V .

In this work we wish to treat and discuss the three factorization methods in a unified way. Thus, for the remainder of this dissertation we adopt the following conventions:¹.

¹I should probably use bold font for X, W and H matrices

Expression matrix: X ($M \times N$)

Metagene matrix: W ($M \times K$)

Metasample matrix: H ($K \times N$)

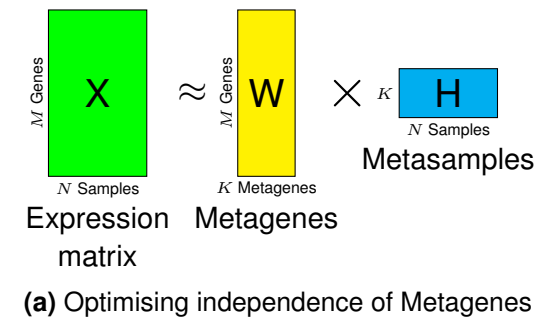
where N is the number of patients (or samples), M is the number of genes and K is the factorization rank, i.e. the number of components or factors. Thus the factorization is written

$$X \approx WH \quad (1)$$

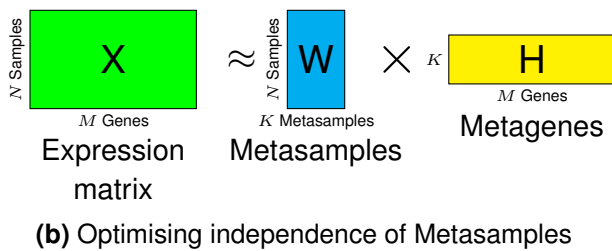
Adding subscripts to indicate the row/column orientation of the matrices:

$$X_{M,N} \approx W_{M,K} H_{K,N} \quad (2)$$

as illustrated in figure 2 (a).



(a) Optimising independence of Metagenes



(b) Optimising independence of Metasamples

Figure 2: Two ways of configuring matrix factorization in the context of gene expression analysis. In configuration (a) NMF and ICA will optimise the *metagenes*, while in (b) the *metasamples* are optimised.

In the case of NMF and ICA, the W and H matrices cannot be trivially exchanged and transposed. This is because the optimisations (sparsity and independence respectively) which define these algorithms are focussed on the W matrix. It is perfectly possible to apply these algorithms to gene expression analysis with exchanged and transposed meanings of W and H , and this is illustrated in figure 2 (b). In this case it is the properties of the *metasamples* which will be optimised. Thus, the two forms are different in substance, not simply in notational convention.

There seems to be substantial confusion and lack of clarity in the way that matrix factorization, particularly ICA, is applied in transcriptomics research. “Surprisingly, both ways of applying ICA to omics data are wide-spread, and sometimes it makes an effort to figure out in which way ICA was applied.” [5], and “Different protocols to apply ICA to transcriptomic data exist and currently no single standard approach has been defined. The main difference in the existing approaches consists in what is considered as source signal matrix in the decomposition” [6]. According to Cantini *et al* references [7], [8], [9] and [10] optimise metagenes, while references [11] and [12] optimises metasamples.

1.1.1 Determining the optimum number of factors

The number of factors, or rank K , to extract is a key decision in any matrix factorization approach. In this regard, PCA differs from ICA and NMF. In PCA it is reasonable to extract all factors, setting $K = N$, the factors being ranked by the associated eigenvalue which also ranks the proportion of variance explained. However, that approach is not valid for ICA and NMF, since differing sets of factors will be obtained for different K , and for a given choice of K all factors are equally important – they do not rank [2].

The problem of determining the optimal K for a given expression matrix is addressed by Kairov *et al* [8], based on optimizing the *stability* of the components over multiple algorithm initializations.

1.2 Gene expression in HGSOC

This section focusses on biological and clinical conclusions relating to gene expression in HGSOC and mentions analysis techniques only in passing.

Obesity is known to negatively impact prognosis in ovarian cancer [13], [7]. Cuello *et al* [13] used NMF based clustering on mRNA microarrays and reverse-phase protein arrays to demonstrate an association between cancer driver genes and obesity related genes.

Wang *et al* [14] also use NMF clustering to identify five subtypes of HGSOC informative of outcomes: 1:mesenchymal, 2:immunoreactive, 3:proliferative, 4:differentiated and 5:anti-mesenchymal. Subtypes 2, 5 are found to be associated with longer survival.

Mairinger *et al* screened 770 immune related genes to identify 11 differentially expressed

genes associated with response to platinum treatment. They find that expression of HS11B1, DNBT1, CKLF, NUP107, CCL18, LY96, ATG7, SLAMF7, CXCL9 is associated with better survival, while IKBKG and SDHA associate with poor survival.

BRCA1 inactivation is known to cause chromosomal instability in many cancers. Pradhan *et al* [15] investigated the role of BRCA1 in HGSOC by copy number and expression analysis, finding surprisingly that inactivation has no relationship with gross genomic alteration. They leave open the question whether DNA repair by PARP plays a role. The relationship between BRCA1/2 and DNA repair – specifically homologous repair deficiency (HRD) – is picked up by Ewing *et al*[16]. They study the complex interplay of single nucleotide variants and large structural variants as they impact BRCA1/2 disruption and thence HRD. This work suggests that when BRCA1/2 loss is detected in HGSOC patients, there may be a clinical role for PARP inhibitors, since this would prevent error-prone non-homologous repair by PARP, and so selectively kill BRCA1/2 disrupted cells.

Note that several of the studies reviewed here use data from the Australian Ovarian Cancer Study (AOCS): [17, 18, 16, 19, 13, 7].

Stratification of HGSOC by immunohistochemistry addresses Kamble *et al*. [20]. They identify a panel of six biomarkers – TCF21, E-cadherin, PARP1, Slug and AnnexinA2. These markers allow stratification into categories including Mesenchymal-to-epithelial transition, Homologous recombination repair and Epithelial-to-mesenchymal transition. This, they argue, allows selection of class-specific inhibitor drugs such as Olaparib and Rucaparib.

The platinum based drug Cisplatin is a key treatment in ovarian cancer, yet tumours often develop resistance, possibly related to the host's immune response. Understanding and predicting such resistance is therefore of clinical importance and is addressed by Maringer *et al* [21] through expression analysis using the NanoString platform with a panel of 770 immune related genes. They find the following to be significantly related to platinum resistance: KLRC1, TCF7, CD274, HSD11B1, COLEC12, PDGFC, FCF1, BMI1, TNFRSF9, ATG10, EWSR1.

A recent pre-publication develops a pipeline for sub-type prediction with the potential to be used clinically [22]. The NanoString gene expression platform is used. See figure 3, their strategy was to focus on small set of 513 genes (vs ~20,000 protein coding genes) known from the literature to have relevance to subtyping. Two approaches were followed by different teams. “All Array”: used expression array data from 1650 patients across 14 studies evaluating 9 supervised learning algorithms by bootstrap, selecting an AdaBoost -like method. “TCGA” used 434 patients from

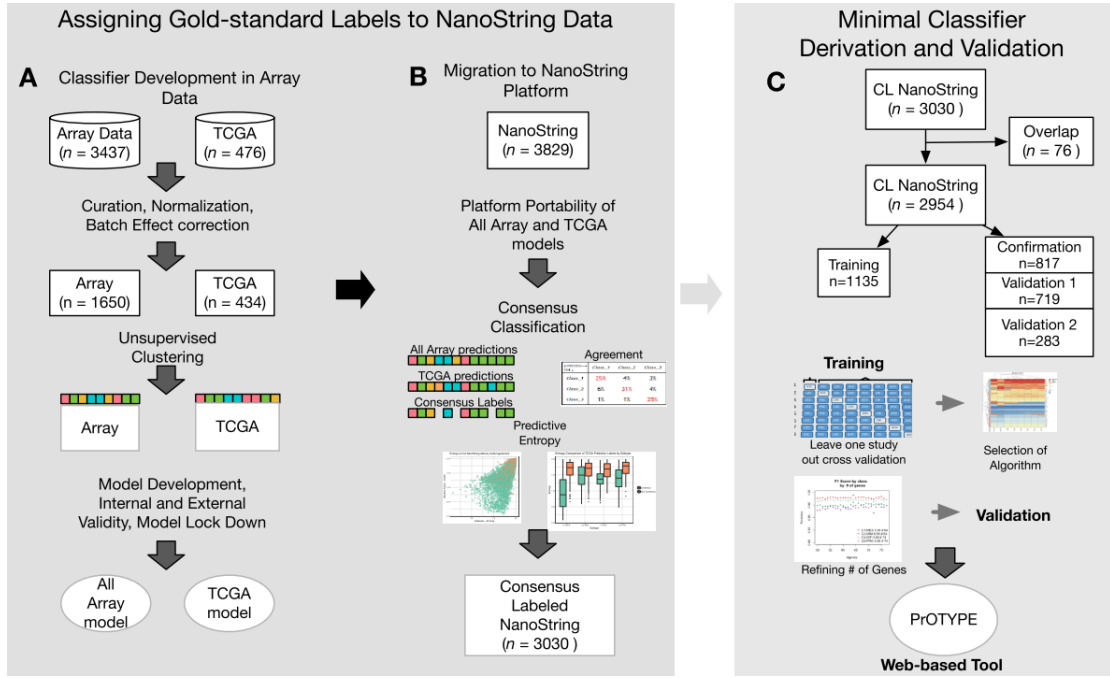


Figure 3: HGSOC subtype prediction by expression analysis of a focussed gene set and consensus across two independent pipelines. From [22].

TCGA evaluating 5 algorithms by cross-validation selecting a random forest. "All Array" had the advantage of more data but needed attention to batch effects. A final classifier took a consensus of the two methods based on a minimal gene set (order 40 genes), validated by a leave-one-out (patient level) approach. Survival analysis was carried out stratified by predicted subtype.

1.3 Research questions

The following research goals were set out early in project.

1. Which are the influential genes in HGSOC according to gene expression data? Do these confirm published results?
2. Which of PCA, ICA and NMF is best suited to this analysis?
3. For identified genes, what is the underlying biology?
4. Can we discriminate subtypes of HGSOC from expression data?
5. Is there value in incorporating somatic and germline genomic data?

2 Methodology

2.1 Outline

Our overall approach is to use *unsupervised* machine learning methods to represent gene expression data in a small number of features, then to study whether these features correlate with clinical and biological variables. This is appropriate in our case, since of the two datasets available (described below), one (TCGA) has relatively large n but little available metadata, while the other (AOCS) is much smaller but has useful metadata. This motivates an approach of unsupervised learning on the TCGA dataset.

2.1.1 Datasets

Two gene expression datasets were assailable for this work (n refers to number of patients, g refers to number of genes).

1. The Cancer Genome Atlas (TCGA) derived, $n=274$, $g=19,601$, with metadata on survival
2. Australian Ovarian Cancer Study (AOCS) [18], $n=80$, $g=19,730$, with metadata on survival, cellularity and additional genomic features.

TODO: *more explanation of the provenance of these datasets.*

2.1.2 Method outline

An overview of the methodology adopted in this work is shown in figure 4.

In outline our method is follows:

1. Identification of a consistent gene set between the TCGA and AOCS datasets.
2. Unsupervised metagene extraction by matrix factorization methods : NMF, ICA and PCA.
3. Metagene selection for robustness by k-means clustering of bootstrap resampled factorizations evaluated by silhouette score, based on the TCGA dataset.

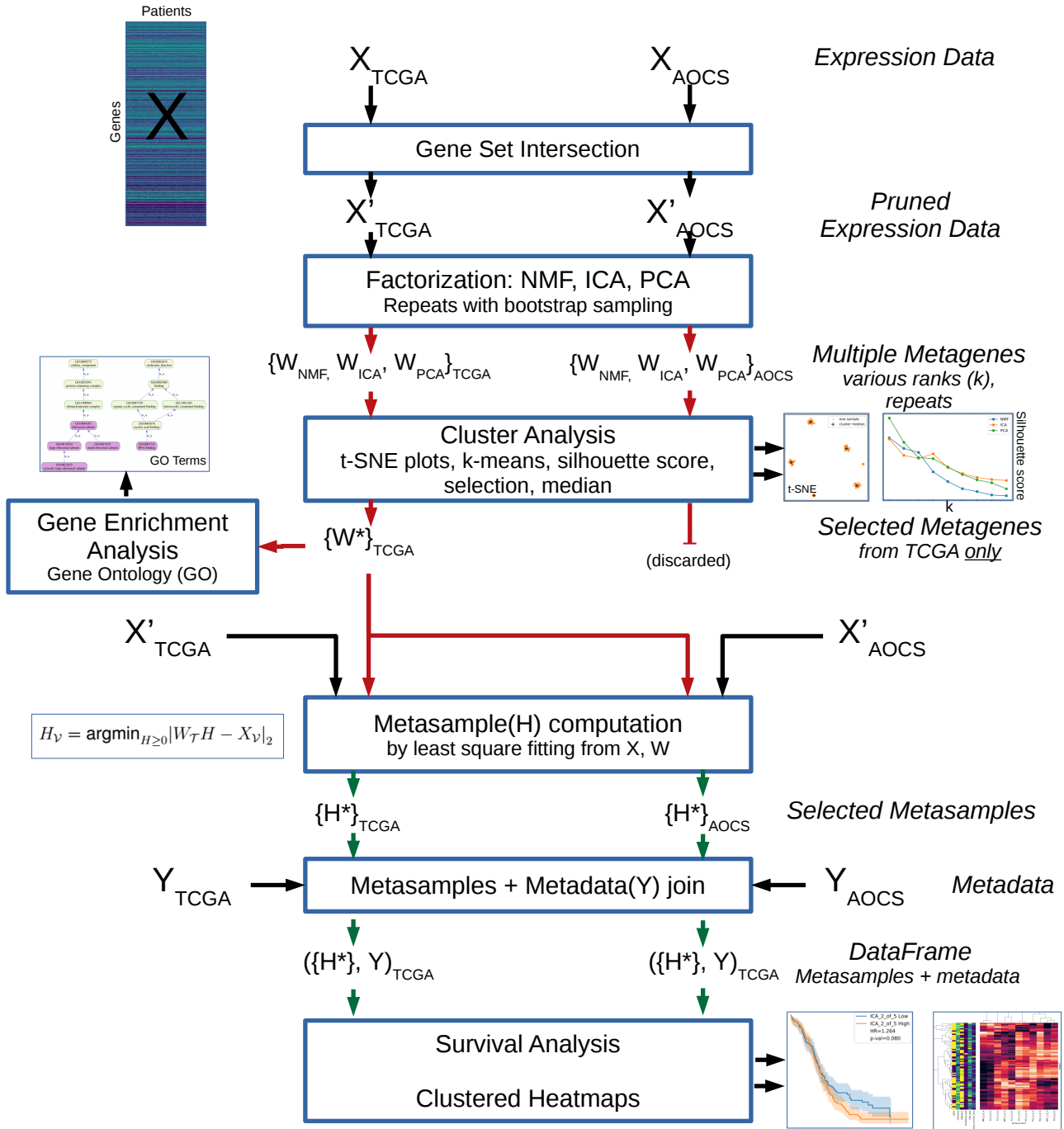


Figure 4: Overview of methodology as information flow. The diagrammatic convention here is that at each stage, both datasets – TCGA and AOCS – are processed separately by the given algorithm. The exception is Gene Set Intersection, which involves interaction between the datasets.

4. Investigation of biological significance of determined factors by gene enrichment analysis against the Gene Ontology (GO).
5. Computation by least squares optimisation of metasamples associated with each TCGA derived metagene against TCGA and AOCS datasets.
6. Alignment of available metadata with computed metasamples, for TCGA and AOCS.
7. Survival analysis on TCGA and AOCS to investigate relationship between metasamples and patient survival.
8. Clustered heatmaps to visualise relationships between metasamples, patients and metadata.

2.1.3 Tools

- Python 3.6
- PyCharm IDE
- Numpy for high performance matrix manipulation
- Pandas for data frame handing
- Matplotlib for general plotting
- Seaborn for heatmaps
- Scikit-learn for matrix factorization and k-means clustering
- GOATOOLS package for gene enrichment analysis against GO
- Lifelines package for survival analysis.

A full list of software and libraries used, with versions, is given in appendix 6.3.

2.2 Data normalization and quality control

Expression data for the AOCS and TCGA datasets was received for this project in a spreadsheet format, having been derived from the RNA-Seq data as described in [16], including normalization by variance stabilizing transformation.

2.3 Gene set intersection

In order to allow factorizations found in the TCGA dataset to be applied to the AOCS dataset it is necessary (or at least convenient) to synchronize the set of genes over which the expression matrices are defined. As provided to this project, the TCGA and AOCS datasets cover 19,610 and 19,730 protein coding genes respectively, 19,566 of which are common to both (according to ENSG encodings). Thus, both datasets were pruned to the 19,566 intersection set and ordered consistently.

2.4 Matrix factorization computation

One of the aims of this work is to compare the efficacy of three methods of dimensionality reduction – NMF, ICA and PCA – as explained in the introduction. The three methods have different properties and notational conventions, but to simplify the discussion here we adopt the notation $X \approx WH$ for all three methods, where X is the (genes, patients) expression matrix W is the (genes, factors) metagenes matrix and H is the (factors, patients) metasamples matrix.

Some of the key algorithm hyper parameters of each method were investigated and tuned with respect to reconstruction accuracy, specifically the root-mean square (RMS) difference between X and WH . The following parameters were explored in each case:

NMF: Parameters `max_iter` (algorithm iterations) and `tol` (tolerance of convergence) were optimised for good accuracy and acceptable execution time. Other parameters of interest are `alpha` (multipluer for regulation term) and `l1_ratio` (multiplier for L1 regularization, when $\text{alpha} > 0$). L1 regularization favours elements being precisely zero, whereas L2 regularization will encourage them to be small. These parameters have not been explored in this project, and the default `alpha = 0` (no regularization) was used.

ICA: Parameters `max_iter` and `tol` were investigated as for NMF above. Additionally, options for the entropy functional which forms the basis of the optimization were investigated.

PCA: This is in principle a deterministic algorithm based on eigenvector decomposition. However, `sklearn.decomposition.PCA` uses a more efficient ‘randomized’ algorithm when the given matrix is larger than 500 in both dimensions. Thus in our use case PCA is seen to have stochastic behaviour.

2.5 Metagene selection by cluster coherence

Deciding on the number of components (factors, metagenes) to extract – that is the factorization rank – is key. Taking more components results in more accurate representation of the observed expression matrix and provides more avenues to explore the underlying biology. However, it is important that the metagenes are *stable*, that is that they have reliable meaning when transferred to other datasets. There are two sources of variation or instability to consider.

Firstly, NMF and ICA are inherently stochastic algorithms, sensitive to their starting state, so repeated runs give different results.

A second and more fundamental source of variation of relevance to all three factorization methods is *sampling error*. Our factorizations are based on a small ($N = 80$ or $N = 374$) sample of patients drawn from the population of HGSC patients; our particular datasets are just two examples of many different ‘draws’ which could have been made from that population.

Bootstrap sampling (also known as *Monte Carlo simulation*) is a common method of empirically propagating the consequence of sampling error when the distribution or processing operations are difficult to model mathematically. This is implemented by performing factorizations multiple times, at each iteration choosing N samples from the N available *with replacement*. For this work 50 repeats were performed, being a compromise between achieving an adequate simulation without overly burdensome computation time. The overall process is summarised as pseudocode in figure 5.

A complication arises in the computation of ICA and PCA factorizations, in that essentially the same factor can arise as w or $-w$ vectors – i.e. 180° rotated. These would appear as separate clusters in repeated sampling, and confound attempts to collect and aggregate. The solution adopted here is to normalise each factor by requiring that the most extreme element – i.e. having the greatest absolute value – is positive, the whole factor being negated if this is not the case. This is arguably over simplistic, but seems to be effective in practice.

Each of the three factorizer methods was evaluated for rank k between 2 and 10. In each case, 50 iterations of factorization are performed on bootstrap samples, generating $50k$ instances of 19,566 dimensioned metagenes. Two dimensional t-SNE plots were generated for visualization purposes. If sampling and algorithm initialisation error are modest then we expect to see k tight clusters of points. To avoid lengthy computation in the t-SNE clustering, the metagenes were first reduced to $r = 20$ dimensions by PCA; brief experiments showed that this reduction had negligible

effect on the t-SNE visualisation for $r \geq 10$.

In order to obtain median estimates of the k metagenes from the $50k$ which were generated, k-means clustering was performed in the PCA reduced (20 dimension) space, delivering k sets of points. These were referenced back to the original 19,566 dimensioned metagenes and the per-dimension median calculated. These k median metagenes were saved to a file named for the specific factorizer and rank k .

The k-means clustering further allowed for a quantitative assessment of cluster coherence for the particular choice of factorizer and rank, via the *silhouette score*. In brief, this is a measure of how close (by Euclidean distance) each point in a cluster is to other points in the cluster versus points *not* in the same cluster. See [Wikipedia: Silhouette \(clustering\)](#). The score is in the range -1 to +1, with 0 implying random scatter and 1 implying all points of a cluster perfectly overlay.

The t-SNE plots and silhouette scores were assessed visually (see figures 7 to 9) to decide, for each of the three factorizers, the highest rank with good cluster coherence, those median metagenes to take forward to gene enrichment and survival analysis. Note that the t-SNE plots are used only for visualisation; they are not involved in the computation of median metagenes or silhouette score.

Initial investigation on the N=80 AOCS dataset showed very poor cluster coherence, even for $k=2$. Thus it was decided to compute and select metagenes only from the N=374 TCGA dataset. The selection rationale is set out in the results section, but is convenient to state here that the following ranks were selected: $K_{\text{NMF}} = 3, K_{\text{ICA}} = 5, K_{\text{PCA}} = 3$. Thus, there were $3 + 5 + 3 = 11$ metagenes taken forward for follow-on analysis.

2.6 Gene enrichment analysis

The metagenes extracted by the above described factorization and clustering process provide valuable information into which genes vary in expression in the study samples; thus in our case, which genes are influential in HGSOC. In order to gain insights into what biological processes are involved, gene enrichment analysis against the Gene Ontology (GO) was carried out for each of the 11 metagenes individually.

The essence of gene enrichment analysis is to compare a candidate set of genes with many functional gene sets, asking the question “are there significantly more (or less, i.e. depletion) intersecting genes than would be expected for the same number of genes being drawn at random

```

for factorizer in NMF, ICA, PCA:
    for k in 2..10:
        Ws = []
        for j in 1..50:
            X = bootstrap sample N from N
            W, H = factorizer(X, rank=k, seed=j)
            append W to Ws

        # Ws is a list of 50*k metagenes, each of length 19,566
        # Pragmatically reduce metagenes to 20 dimensions by PCA

        Ws_reduced = PCA(Ws, rank=20)
        plot t-SNE(Ws_reduced)
        clustering = k-means clustering(Ws_reduced, n_clusters=k)
        score[factorizer, k] = silhouette score(clustering)
        median_metagenes = calculate medians for k clusters of metagenes
        save median_metagenes to file by factorizer and k
        for each factorizer
            plot score vs k

```

Figure 5: Pseudocode for generating median metagenes and assessing their stability to random algorithm initialization and sampling error.

(without replacement) from the total population of genes in the study.

For each metagene, the candidate gene set was determined as those genes having weights outwith three standard deviations of the mean. This set was analysed using the Python GOA-TOOLS package [23].

The gene ontology was downloaded from <http://purl.obolibrary.org/obo/go/go-basic.obo>. (Purl.org is a resource for managing permanent URLs; obo refers to the Open Biological and Biomedical Ontology (OBO)). Annotations linking human genes to GO concepts was downloaded from the GO website, specifically <http://geneontology.org/gene-associations/goa-human.gaf.gaf>. The gene population was defined as the common 19,566 protein coding genes (see section 2.3) against which the metagenes were computed.

Uncorrected p-value threshold was set to 0.01. Multiple hypothesis significance testing used the false discovery rate (FDR) method of Benjamini and Hochberg, the FDR threshold being set to 0.01. This is more stringent than the 0.05 value which is typically used, and was chosen since multiple metagenes are being analysed, implying multiple hypothesis testing over and above that which is accounted for by FDR filtering within a single gene enrichment analysis run.

The result of this analysis, per metagene, is a list of enriched (or depleted, however in our

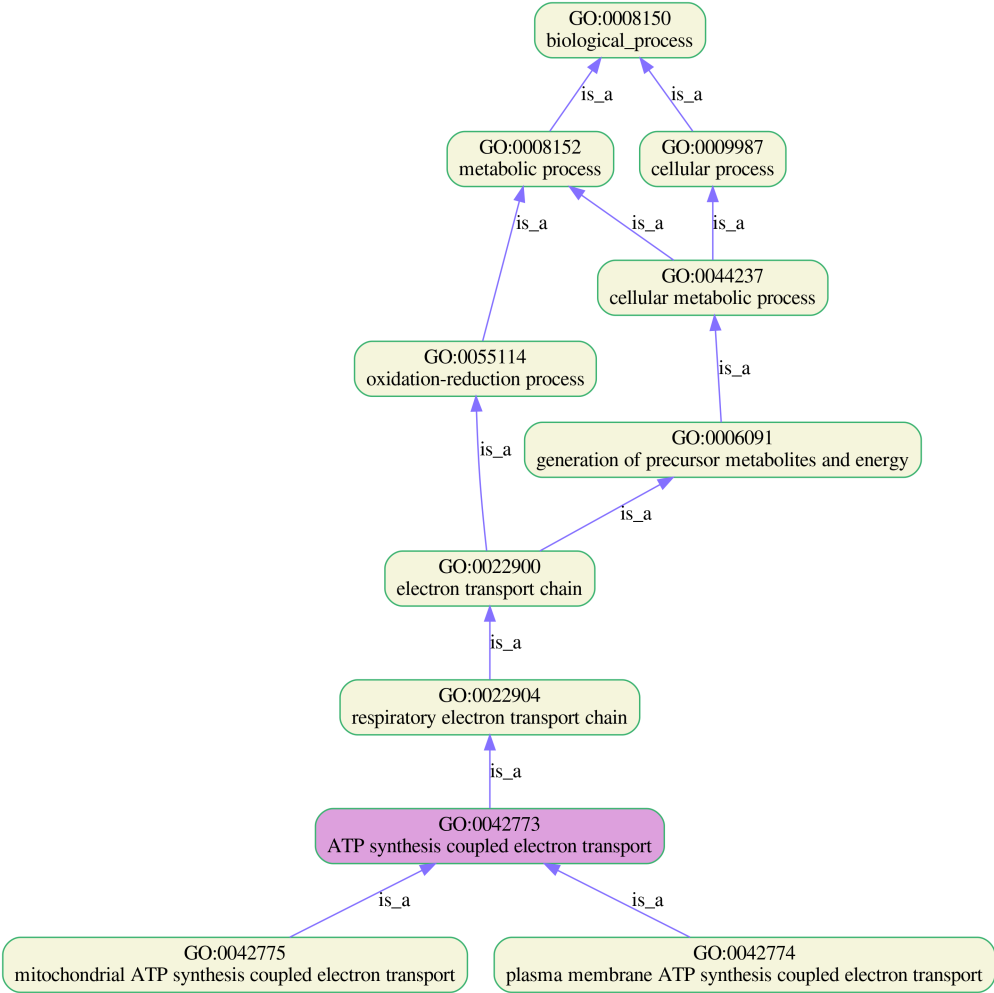


Figure 6: Example of a small section of the Gene Ontology (GO), focussed GO:0042773 (in purple), showing parents and children of the term. Generated by GOATOOLS.

case no depleted terms were found) GO terms, each with an associated list of involved genes and a FDR significance level. This list can be inspected directly for insights, but that misses the point of the GO, which is to organise the terms hierarchically by ‘is a’ relationships. Thus, the enriched terms were rendered graphically to show them in the context of their parent terms.

2.7 Transfer of learned metagenes to novel a dataset

It is fundamental to our approach that metagenes determined on the basis of one cohort of data can be used to generate metasamples for a different cohort. In the exposition below we refer to these as the *training* and *validation* cohorts respectively.

Rank k matrix factorization on the training dataset \mathcal{T} (e.g. TCGA) results in:

$$X_{\mathcal{T}} \approx W_{\mathcal{T}} H_{\mathcal{T}} \quad (3)$$

where $X_{\mathcal{T}}$ is the expression matrix of shape $(g_{\mathcal{T}}, n_{\mathcal{T}})$, with $g_{\mathcal{T}}$ the number genes and $n_{\mathcal{T}}$ the number of patients. $W_{\mathcal{T}}$ is the metagene matrix of shape $(g_{\mathcal{T}}, k)$ and H_t is the metasamples matrix of shape $(k, n_{\mathcal{T}})$.

We wish to apply the factorization learned on \mathcal{T} to a novel dataset \mathcal{V} (specifically the AOCS dataset) of shape $(g_{\mathcal{V}}, n_{\mathcal{V}})$. Importantly, $n_{\mathcal{V}} = 1$ reflects the application of these methods to a single patient in a clinical setting. To apply the learned factorization we need to find $H_{\mathcal{V}}$ as in the factorization

$$X_{\mathcal{V}} \approx W_{\mathcal{V}} H_{\mathcal{V}} \quad (4)$$

In both the experimental and clinical situation we are given $X_{\mathcal{V}}$ but not $W_{\mathcal{V}}$ and require to find $H_{\mathcal{V}}$. We *cannot* simply perform the matrix factorization on dataset \mathcal{V} since $n_{\mathcal{V}}$ may be small, or even a single patient. However, if patients in datasets \mathcal{T} and \mathcal{V} are drawn from the same population (ovarian cancer patients), then $X_{\mathcal{T}}$ and $X_{\mathcal{V}}$ can be expected to have similar distributions w.r.t to their columns, and thus $W_{\mathcal{T}}$ and $W_{\mathcal{V}}$ can be expected to be equivalent within sampling error. This only makes sense if the two expression matrices $X_{\mathcal{T}}$ and $X_{\mathcal{V}}$ are defined over the *same set of genes*, so that $g_{\mathcal{T}} = g_{\mathcal{V}} = g$, in which case $W_{\mathcal{T}}$ and $W_{\mathcal{V}}$ have the same shape of (g, k) .

We thus need to solve for $H_{\mathcal{V}}$ in

$$X_{\mathcal{V}} \approx W_{\mathcal{T}} H_{\mathcal{V}} \quad (5)$$

This can be solved by the method of least squares. In the case that the original factorization was by NMF, we use non-negative least square regression (NNLS):

$$H_{\mathcal{V}} = \operatorname{argmin}_{H \geq 0} \|W_{\mathcal{T}} H - X_{\mathcal{V}}\|_2 \quad (6)$$

where $\|\cdot\|_2$ indicates Euclidean distance or L2-norm. The Python library function `scipy.optimize.nnls` is used.

For ICA and PCA we use ordinary least square regression, formulated above but dropping the $H \geq 0$ constraint, using `scipy.linalg.lstsq`.

The end result of the analysis is the $H_{\mathcal{V}}$ matrix of shape $(k, n_{\mathcal{V}})$, thus delivering for each dataset in our \mathcal{V} a feature vector – or metasample – of length k .

Since in this work we wish to evaluate the efficacy of the three factorization methods – NMF,

ICA and PCA – we in fact take forward three different H matrices, each having ranks as for the associated metagenes.

2.8 Reconciling computed metasamples and metadata

To carry out patient level analysis – survival analysis, heatmaps and boxplot – as described in the following sections, it is necessary to compile tables (Panda DataFrames) which bring together per-patient metasamples relating to each of the selected metagenes, with associated metadata – such as cellularity and survival information. The metagenes always derive from the TCGA dataset (because of its larger size as explained in section 2.5), but we wish to apply these metagenes to the expression data and associated metadata of either the TCGA or AOCS datasets. The mathematics of transferring metagenes across datasets has been described above. Care is required to ensure that expression matrices aligned correctly with metagenes with respect to their genes (rows), and with the metadata with respect to patient identifiers in the columns. Note that the same transferring approach is taken when metasamples are required for TCGA, even though we could in that case obtain the H matrix directly from the factorization.

2.9 Survival analysis

Survival analysis was performed to investigate whether the metasamples derived from the selected metagenes correlate with patient survival. Overall survival (OS) data is available for both the TCGA and AOCS datasets. Additionally, progression free survival (PFS) data is available for AOCS. As described above, metagenes were obtained by factorization on the TCGA dataset only. Application to TCGA (for OS) thus represents an in-sample test, while application to AOCS (for OS and PFS) is a more exacting out-of-sample test. There are thus three analyses to consider: 1) TCGA→TCGA (OS), 2) TCGA→OACS (OS) and 3) TCGA→OACS (PFS).

Analysis was performed using the Python Lifelines package [24]. Metasample values were binarised to 0, 1 by thresholding at the median value. Kaplan-Meier plots were made in respect of derived metasample for each of the three analyses – making 11×3 plots each with two survival curves and showing with 95% confidence intervals. A hazard ratio (HR)² was calculated for each plot by fitting Cox's proportional hazards model with p-value relating to the hypothesis that HR is significantly different to 1.0.

²Do I need to explain the definition and meaning of HR?

2.10 Metasample heatmap analysis

To further investigate the relationship between metasamples and to available patient metadata, clustered heatmaps were generated using the `Seaborn clustermap()` function from the reconciled metasamples and metadata (section 2.8). Heatmaps were generated for TCGA and AOCS datasets (*Should say something about stratifying the metadata, when I figure it out*). Heatmap clustering by correlation distance was applied.

2.11 Codebase

The described method was implemented in Python. All code is available in a github repository: <https://github.com/ipoole/HgsocTromics>. Good software engineering practice has been followed, with an object-oriented design, frequent commits and unit testing. Unit tests are based on tiny expression matrices, just 100 genes by 10 patients, thus the whole test suite of over 60 tests executes in around 30 seconds. These tests are particularly valuable when re-factoring code by providing a rapid means of detecting coding errors. The total codebase is approximately 2,800 lines of Python. All plots are generated in vector graphics pdf format to ensure smooth scaling to any resolution.

3 Results

Results of applying the above described methodology are explained and presented here. Deeper interpretation and discussion is deferred to the following section. Throughout, consistent colours of blue, orange and green are used for results relating to NMF, ICA and PCA respectively. Specific metagenes are referred to by, for example, “NMF-2-of-3” – meaning the 2nd component of the rank $k = 3$ NMF factorization.

3.1 Cluster coherence analysis results

From figure 7 it can be seen that with sampling error excluded, clusters appear reasonably coherent, but when sampling error is modelled by bootstrap sampling then the factorizations become much less stable. This demonstrates that *sampling* error is far greater than errors due to algorithm

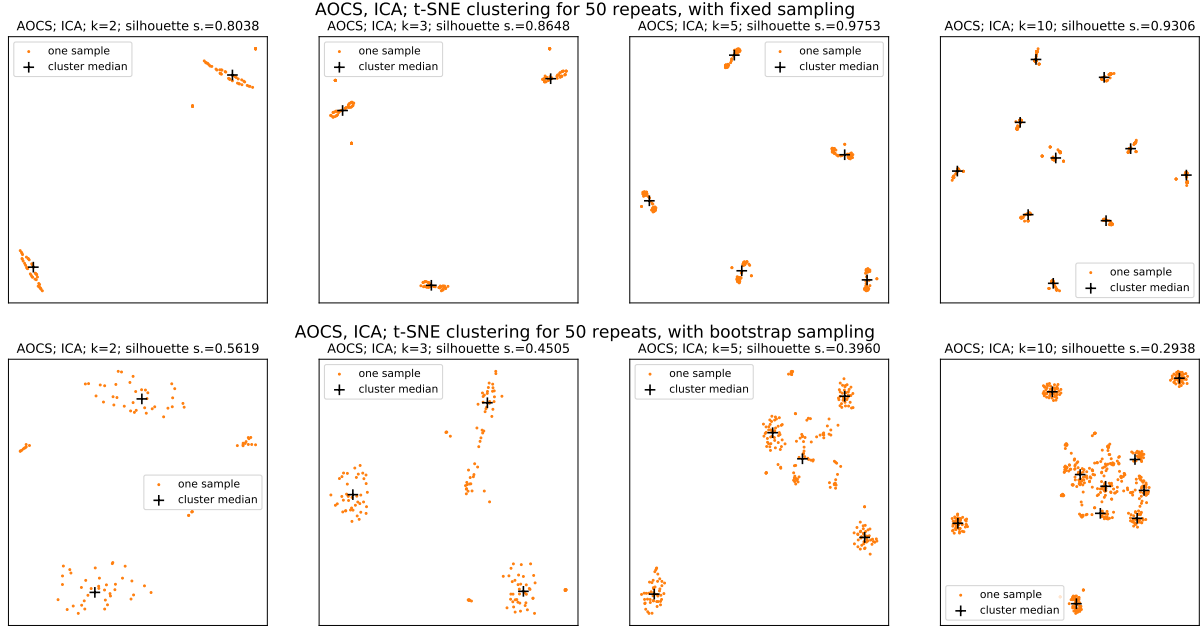


Figure 7: Clustering of metagenes from ICA factorizations on the N=80 AOCS dataset, comparing *fixed* sampling (top row) with *bootstrap* sampling (bottom row) for a selection of factorization ranks.

initialisation when the dataset is small ($N=80$), making metagene extraction unreliable. Figure 8 makes the same comparison for the larger $N=374$ TCGA dataset, in which it can be seen that the impact of sampling error is not so severe. For brevity only results for ICA are shown, but a very similar effect is observable for PCA and NMF.

For this reason, and in line with our overall strategy, it is appropriate to perform all metagene extraction on the larger TCGA dataset, in the expectation that the obtained metagenes will be more robust and likely to better generalise to other datasets.

The critical decision of the choosing the factorization rank for each method – K_{NMF} , K_{ICA} and K_{PCA} – is based on figure 9. On this bases, considering both the t-SNE plots and silhouette scores, the following choices were made: $K_{\text{NMF}} = 3$, $K_{\text{ICA}} = 5$, $K_{\text{PCA}} = 3$.

The rationale for these choices is that, firstly $k > 2$ is desirable to have sufficient information to work with. NMF cluster coherence seems to deteriorate after $k = 3$. Looking at the graph of silhouette scores (figure 9, bottom), ICA appears to have a sweet spot at $k = 5$. For PCA, $k = 3$ or 4 both seem reasonable; $k = 3$ was selected.

There is a curious artefact visible in the NMF factorization clusterings of figure 9, top row. For $k = 2, 3$ and 5 several of the clusters show a bi-modal character. This is not observed in the fixed sampling case (not shown). The artefact is difficult to explain. It cannot be the 180° rotation issue discussed earlier, since this does not apply to the all +ve components.

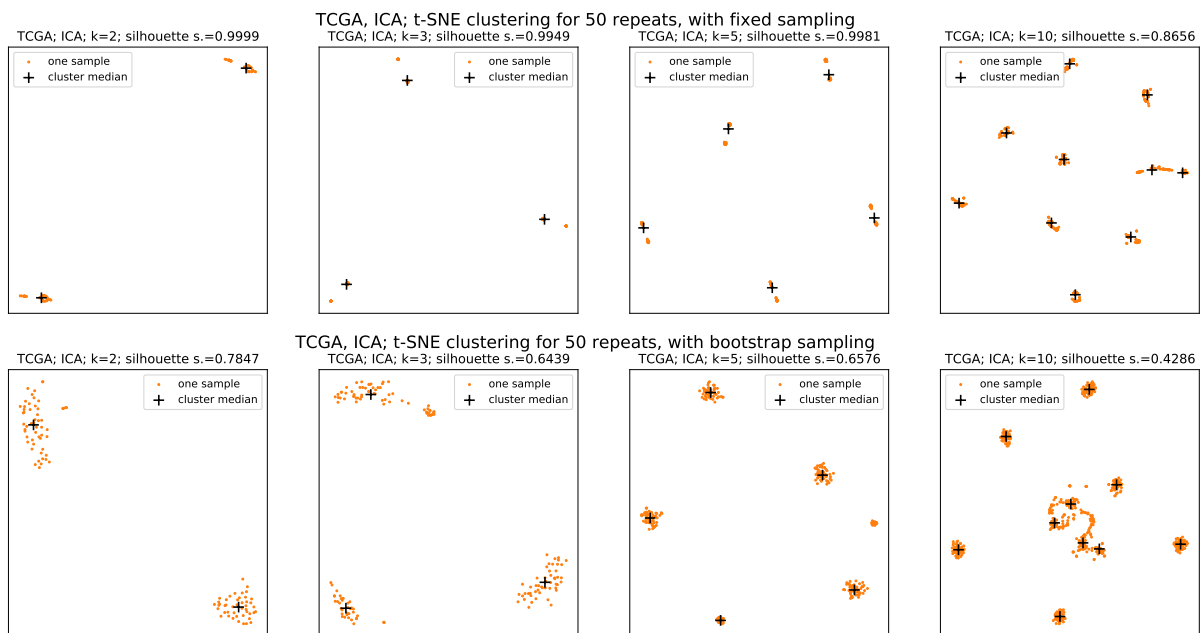


Figure 8: Clustering of metagenes from ICA factorizations on the N=374 TCGA dataset, again comparing fixed and bootstrap sampling.

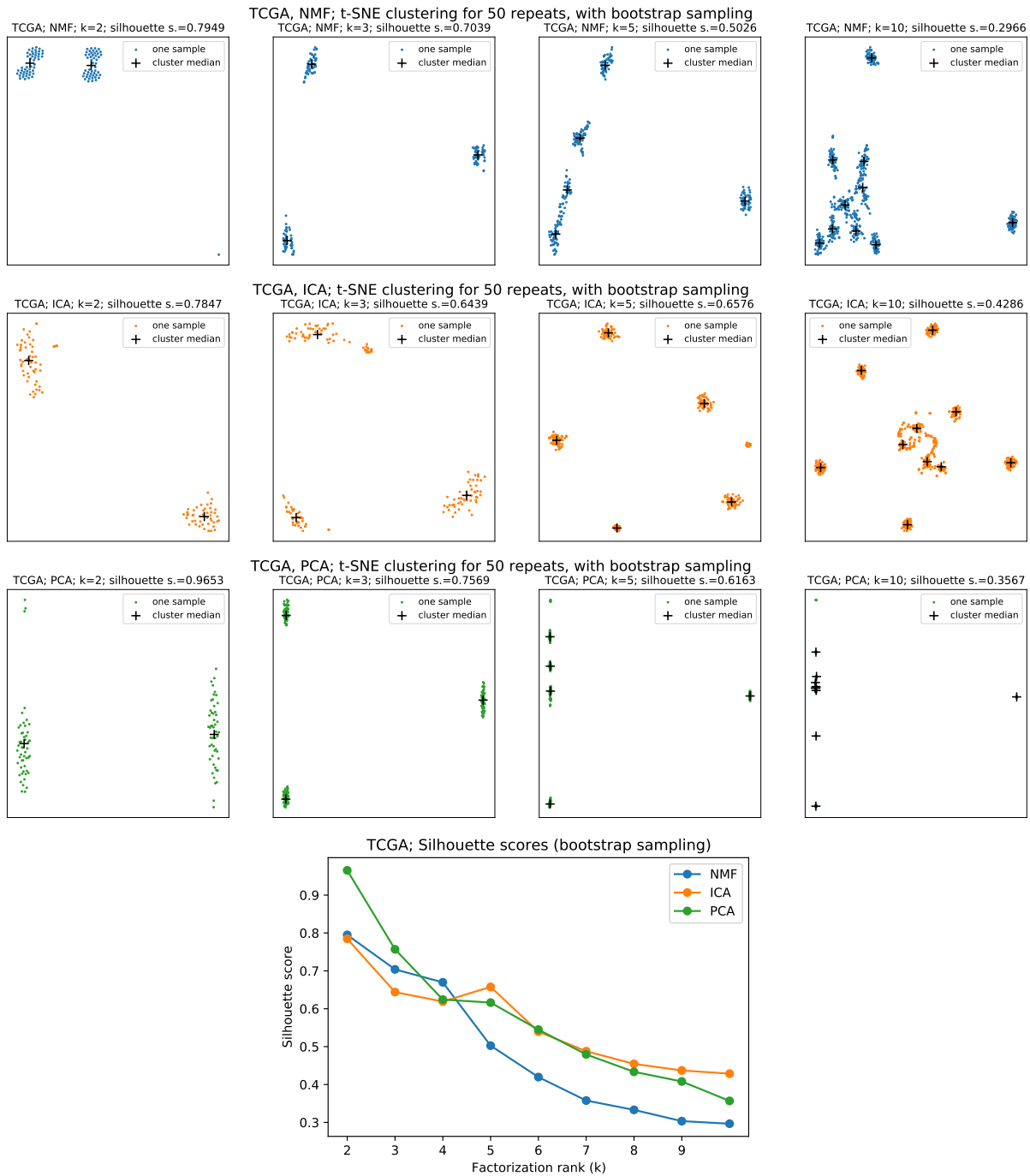


Figure 9: Metagene clustering for all three methods applied to the N=374 TCGA dataset with bootstrap sampling, over a range of factorization ranks. The silhouette scores are also plotted (bottom). It is on the basis of this figure that the factorization ranks for each method were selected.

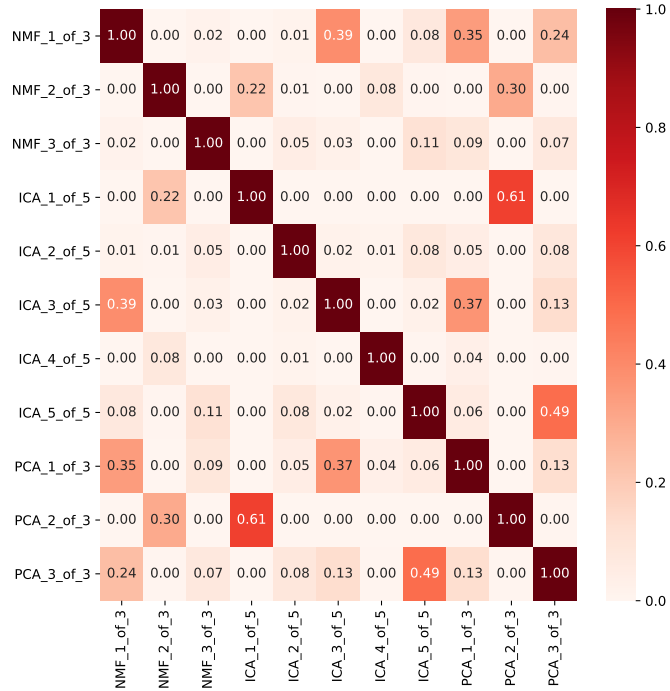


Figure 10: Heatmap of Jaccard similarities between the candidate genes identified by the 11 components.

3.2 Gene Enrichment (against GO) Results

Gene enrichment analysis against the GO results in, for each of the 11 metagenes, a table of GO terms with a list of the candidate genes which have an annotated association to that term. To take full advantage of the hierarchical nature of the GO, results are presented as lineage maps in figures 11 to 14. The contributing candidate genes for all significantly enriched terms are shown beneath each figure. (Ideally, the specific genes would be listed alongside each term, but this is difficult to achieve graphically). High-level terms at depth less than 3 were removed, since these are generic (e.g. "regulation of biological process") and so uninteresting. One component – ICA-4-of-5 – was problematic in that 49 GO terms (with depth ≥ 3) were identified as significant. For this component it was necessary to limit the graphic to the 12 terms having the largest number of associated candidate genes. The full table of terms for this component is available in appendix 6.2.

The four components NMF-3-of-3, ICA-1-of-5, ICA-2-of-5 and PCA-2-of-3 yielded no significant enriched terms (for FDR ≤ 0.01).

To what extent do the 11 components overlap in the candidate genes they propose (independent of enrichment analysis)? Figure 10 shows this by a heatmap of Jaccard similarities. Jaccard

similarity (or index) is defined on a pair of sets, in this case sets of genes, as:

$$\text{Jaccard}(A, B) = \frac{A \cap B}{A \cup B}$$

lying between 0 (no similarity) and 1 (identical).

From this heatmap we can see that within a factorization method the components have almost no similarity – they represent largely independent projections, as one would expect. Between methods, however, there is considerable overlap in some cases. In particular PCA 2_of_3 vs ICA 1_of_5 ($J=0.61$), PCA 3_of_3 vs ICA 5_of_5 ($J=0.49$) and NMF 1_of_3 vs ICA 3_of_5 ($J=0.39$).

3.3 Survival analysis results

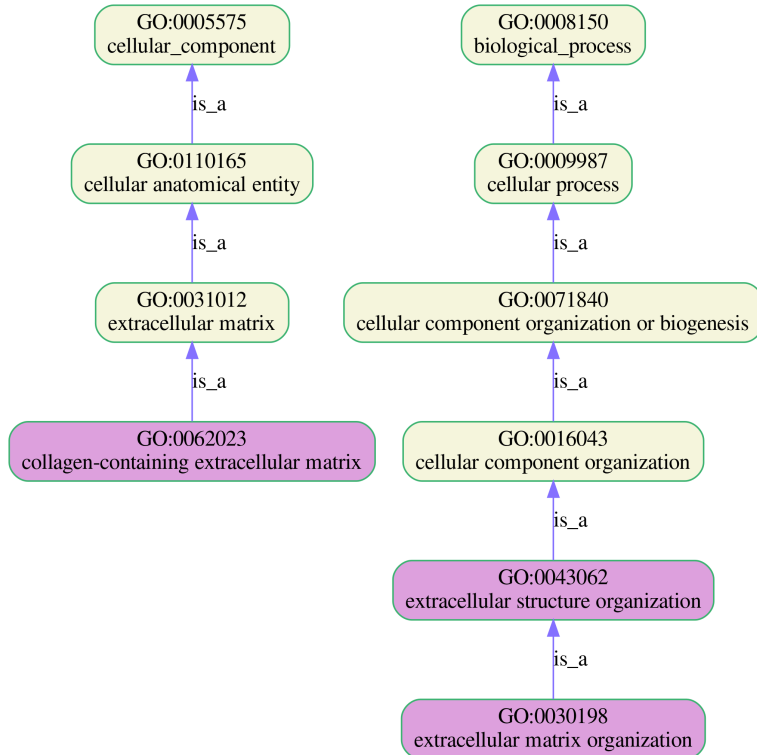
Kaplan-Meier overall survival (OS) plots stratified by each metasample component are shown for the TCGA dataset in figure 15 and for the AOCS dataset in figure 16. Plots for progression free survival (PFS) on OACS are shown in figure 17. All plots show 95% confidence intervals and hazard ratio (HR) with associated p-value.

All of these results are summarised in figure 18, which brings together the three sets of results – TCGA (OS), OACS (OS) and OACS (PFS) – with respect to the 11 metasample components. \log_2 HR is used in order that the *sense* of the survival impact can be readily appreciated. If a metasample component has a robust correlation with survival, then we expect the p-value for all three sets of results to show significance *and* for the effects to have the same sense – be in the same direction. None of the 11 components pass this test.

The component closest to correlation with survival would seem to be PCA 1-of-3, showing a reasonably consistent hazard ratio of around 1.3 ($2^{0.4}$) across the three experiments. This has $p < 0.05$ in the larger TCGA dataset, but not in the smaller AOCS dataset.

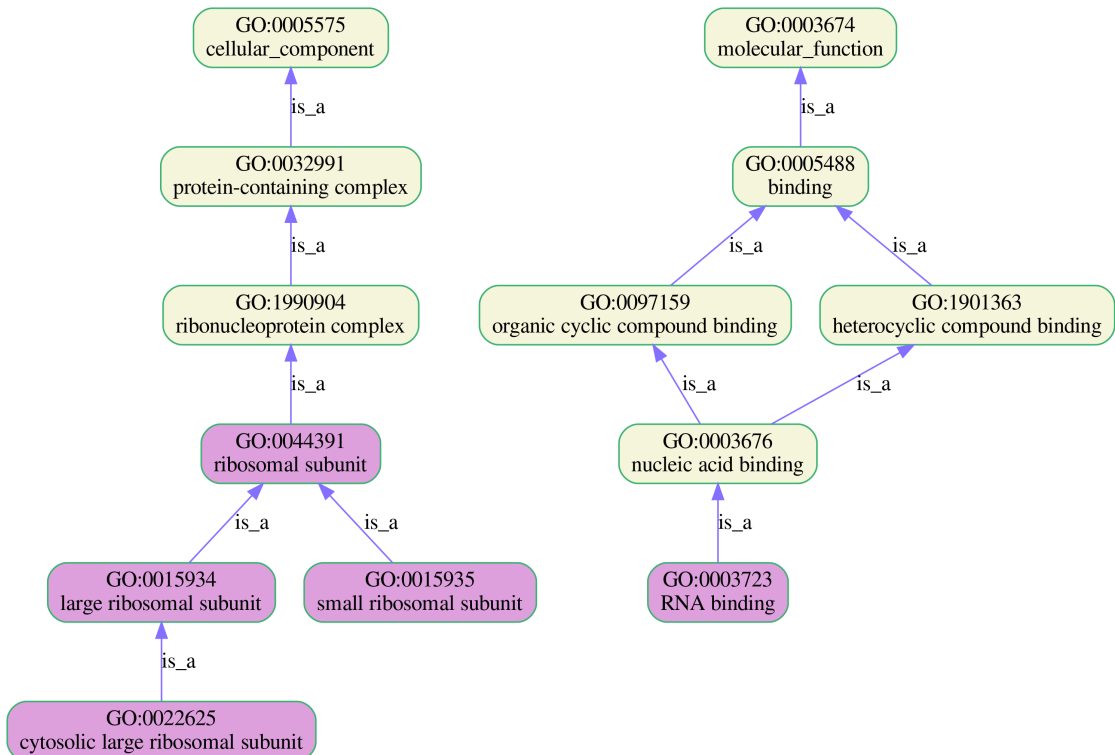
3.4 Metasample heatmap clustering results

As with survival analysis, metasamples were derived from the metagenes factorized from the TCGA dataset, then applied to both TCGA and AOCS. The resulting heatmaps are shown in figures 19 and 20 respectively. Metadata was available for the AOCS dataset, and this is presented in colour coded columns on the left of figure 20. The meanings of each column are as follows:



Genes: EFEMP1 LAMA4 MMP9 ADAMTS2 FGL2 COL6A2 COL16A1 ADAMTS1 MMP19 TNC PCOLCE ECM1 COMP CCDC80 HTRA1 NID2 COL3A1

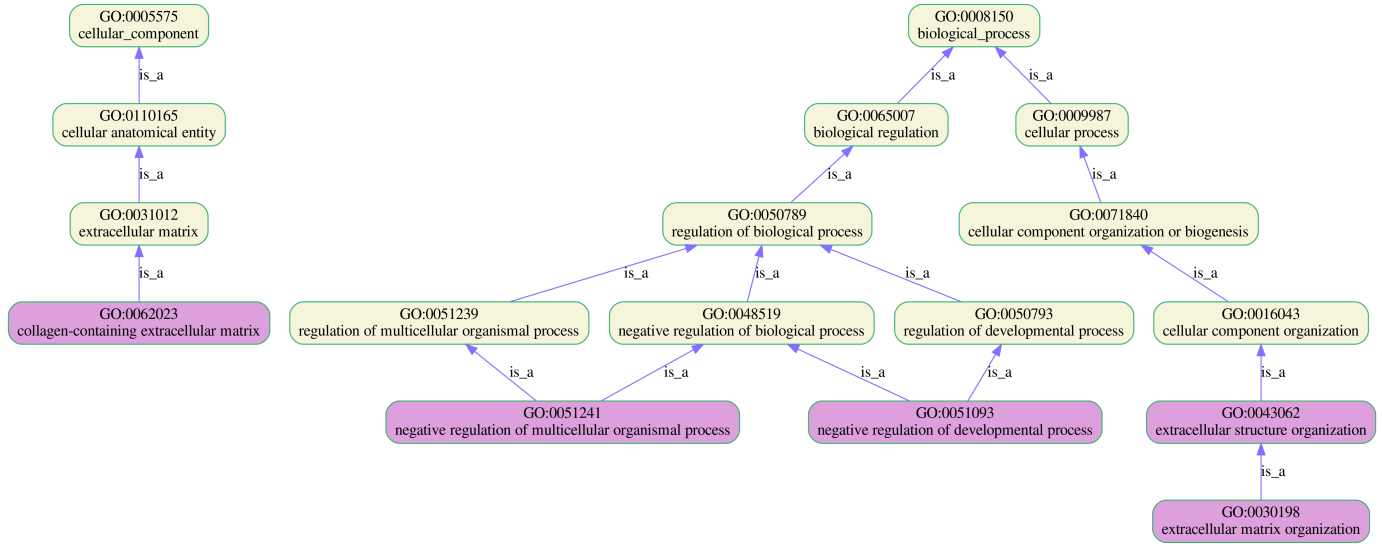
Component NMF-1-of-3



Genes: RPL18A RPS14 RPL13A RPS27 RPL8 RPS4X EEF1A1 RPL28 RPLP0 RPL32 RPL37 RPS11 RPL15 RPS18 RPL13 RPS20

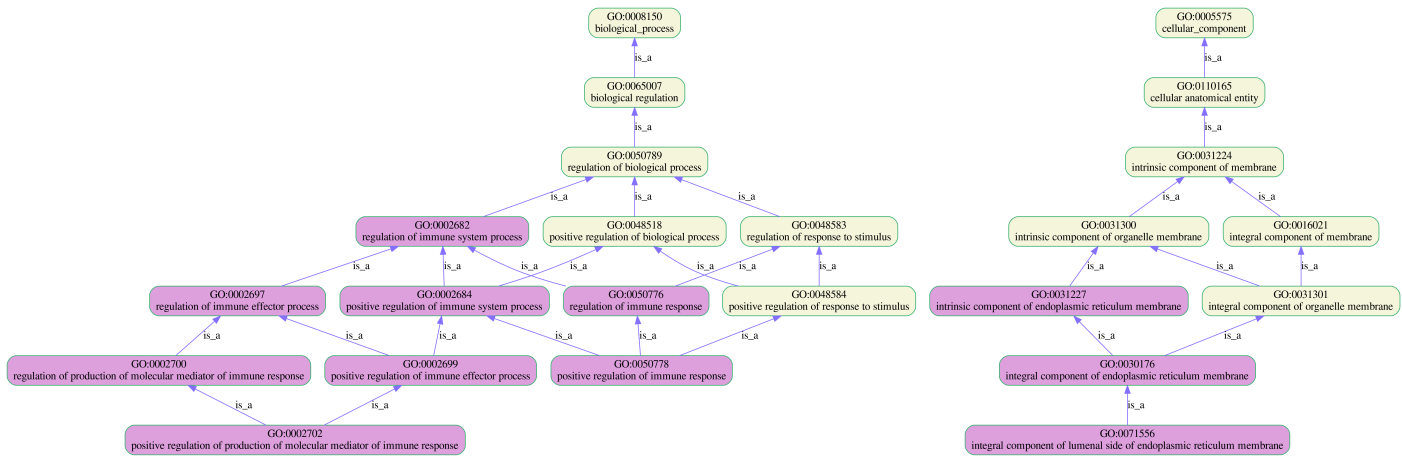
Component NMF 2-of-3

Figure 11: Lineage maps of enriched Gene Ontology (GO) terms for components NMF-1-of-3 and NMF-2-of-3. In these diagrams, enriched terms are coloured purple, while there ancestors in the ontology are yellow. (NMF-3-of-3 produced no significant enrichment results)



Genes: COL26A1 PTGER3 LAMA4 ENPP1 RFLNB COL6A2 ADAMTS16 TMEM176B COL16A1 ADAMTS1 MMP19 MATN3 TNC ADAMTS5 THBS1 TMEM176A ECM1 CCDC80 NID2 COL3A1 THBS2 ADAMTS7 EFEMP1 MMP9 ADAMTS2 COL6A6 DPT OGN PCOLCE PRICKLE1 COMP HTRA1 ISM1 RFLNA

Component ICA-3-of-5



Genes: CD300A HLA-DOA CD38 KLK7 LILRB2 HLA-DRB5 VTCN1 IGLL5 HLA-DPB1 HLA-DMB HAVCR2 HLA-DQA2 HLA-DQB1 SLAMF7 FCGR1A HLA-DPA1 MFAP4 C3 CD74 HLA-DQA1 HLA-DRA FCGR2B SLAMF8 DOCK8 RSAD2 HLA-DQB2 SASH3 HLA-B

Component ICA-5-of-5

Figure 12: Lineage maps of enriched Gene Ontology (GO) terms for components ICA-3-of-5 and ICA-5-of-5

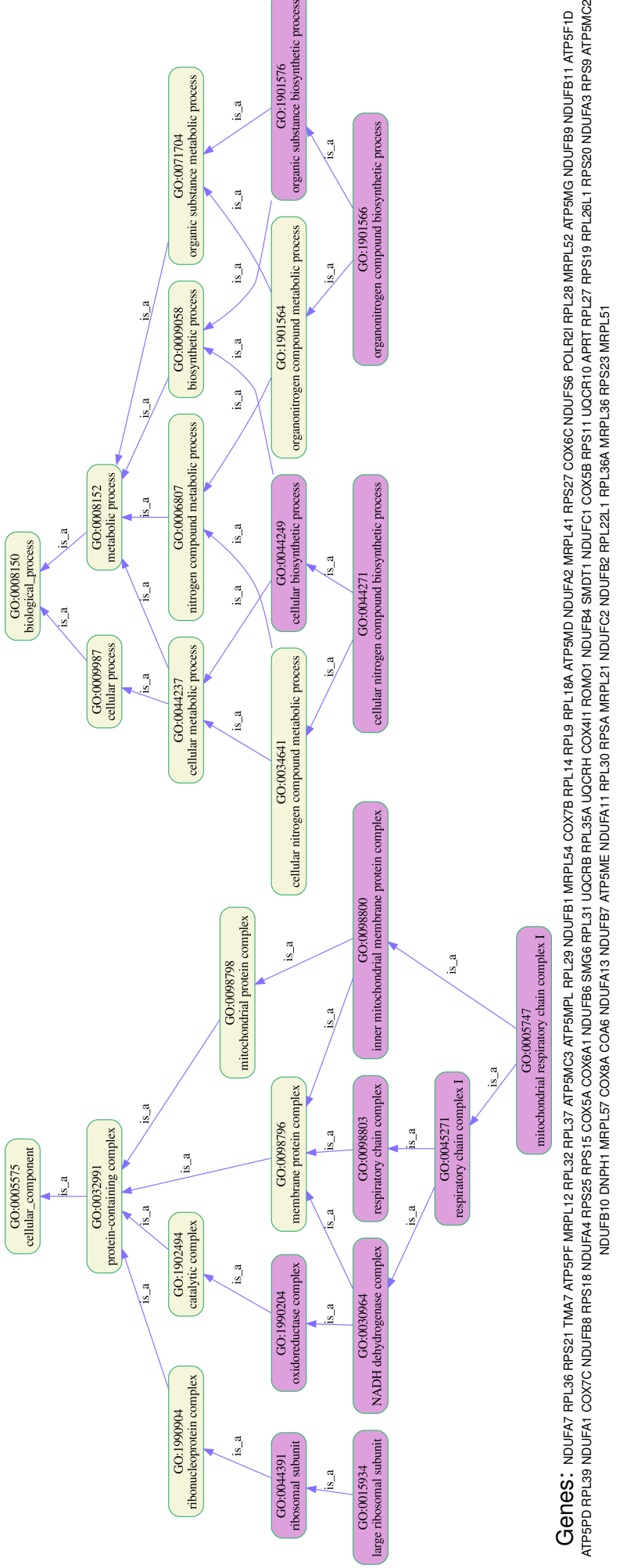
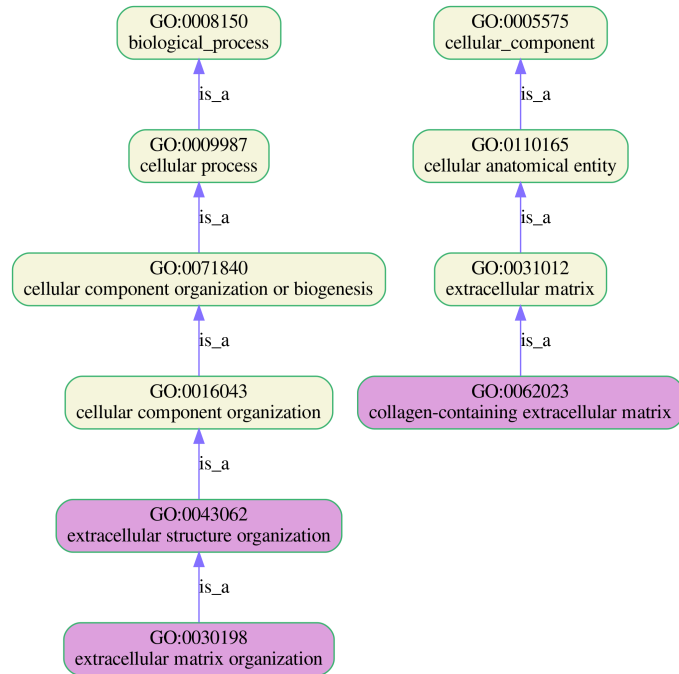
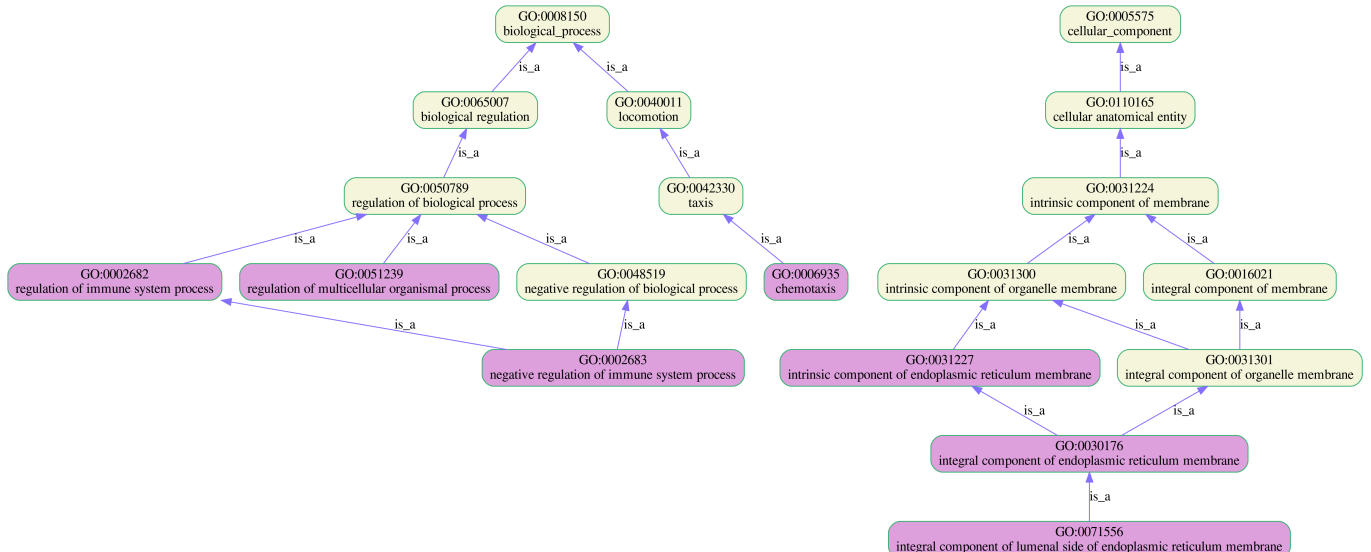


Figure 13: Lineage maps of enriched Gene Ontology (GO) terms for component ICA-4-of-5. For this component it was necessary to additionally filter the enriched terms – see text.



Genes: COL16A1 ADAMTS1 COL26A1 ADAMTS7 TNC PCOLCE ADAMTS2 COL14A1 CCDC80 COMP COL6A2 ADAMTS16 NID2 COL3A1 ADAMTS9 OGN

Component PCA-1-of-3



Genes: CD300A TLR7 KLK7 LILRB2 PTGER3 HLA-DRB5 CXCL9 CCL2 IGLL1 VSIG4 TLR8 HAVCR2 CD2 HLA-DQA2 TMEM176B SLAMF7 HLA-DQA1 CD74 TMEM176A THBS1 CXCR6 ITGAX CXCL1 HLA-DQB2 SASH3 HLA-B HLA-DOA THBS2 VTCN1 PAEP HLA-DPB1 HLA-DRB1 CCR1 PAX2 B2M HLA-DPA1 HLA-DQB1 FCGR1A C3 TYROBP CCL11 HLA-DRA FCGR2B SLAMF8 VSIR

Component PCA-3-of-3

Figure 14: Lineage maps of enriched Gene Ontology (GO) terms for components 1 and 3 from the rank=5 PCA factorization. (Component PCA-2-of-3 produced no significant enrichment results)

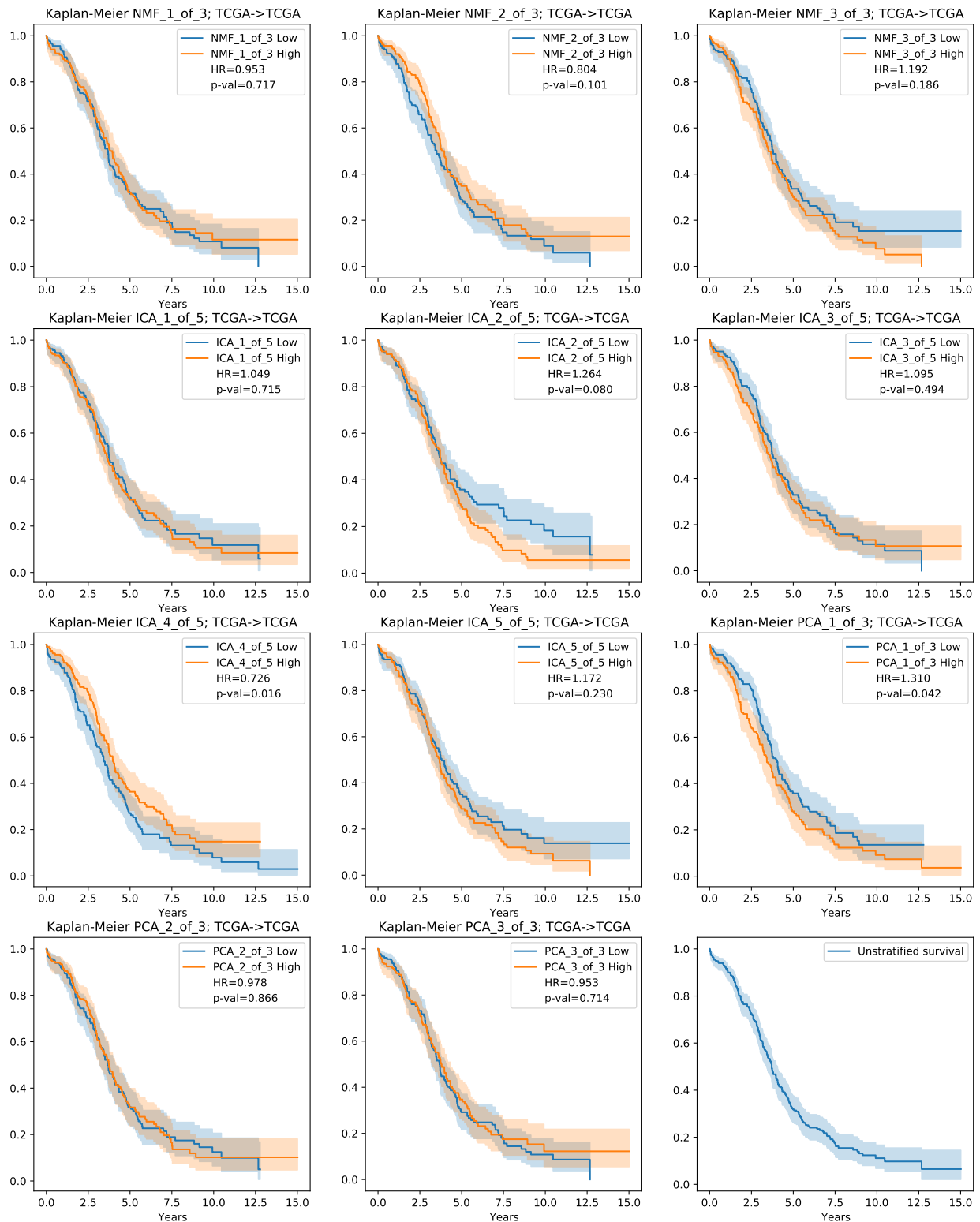


Figure 15: Kaplan-Meier plots for each metasample component, stratified at the median value, for TCGA → TCGA for overall survival (OS) case. Hazard ratio and p-value is shown for each case. The final plot (bottom right) is unstratified overall survival

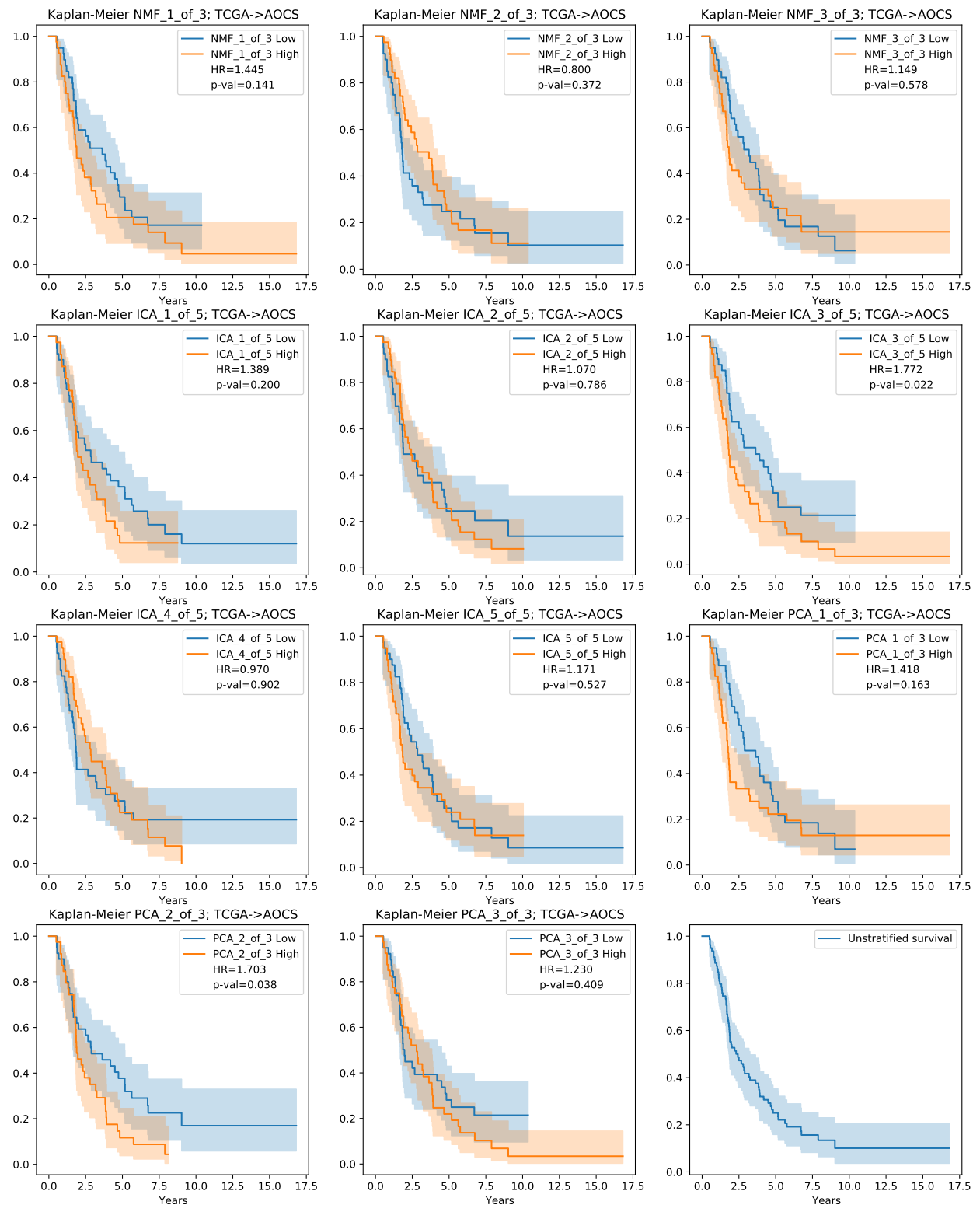


Figure 16: Kaplan-Meier plots for TCGA → TCGA for overall survival (OS).

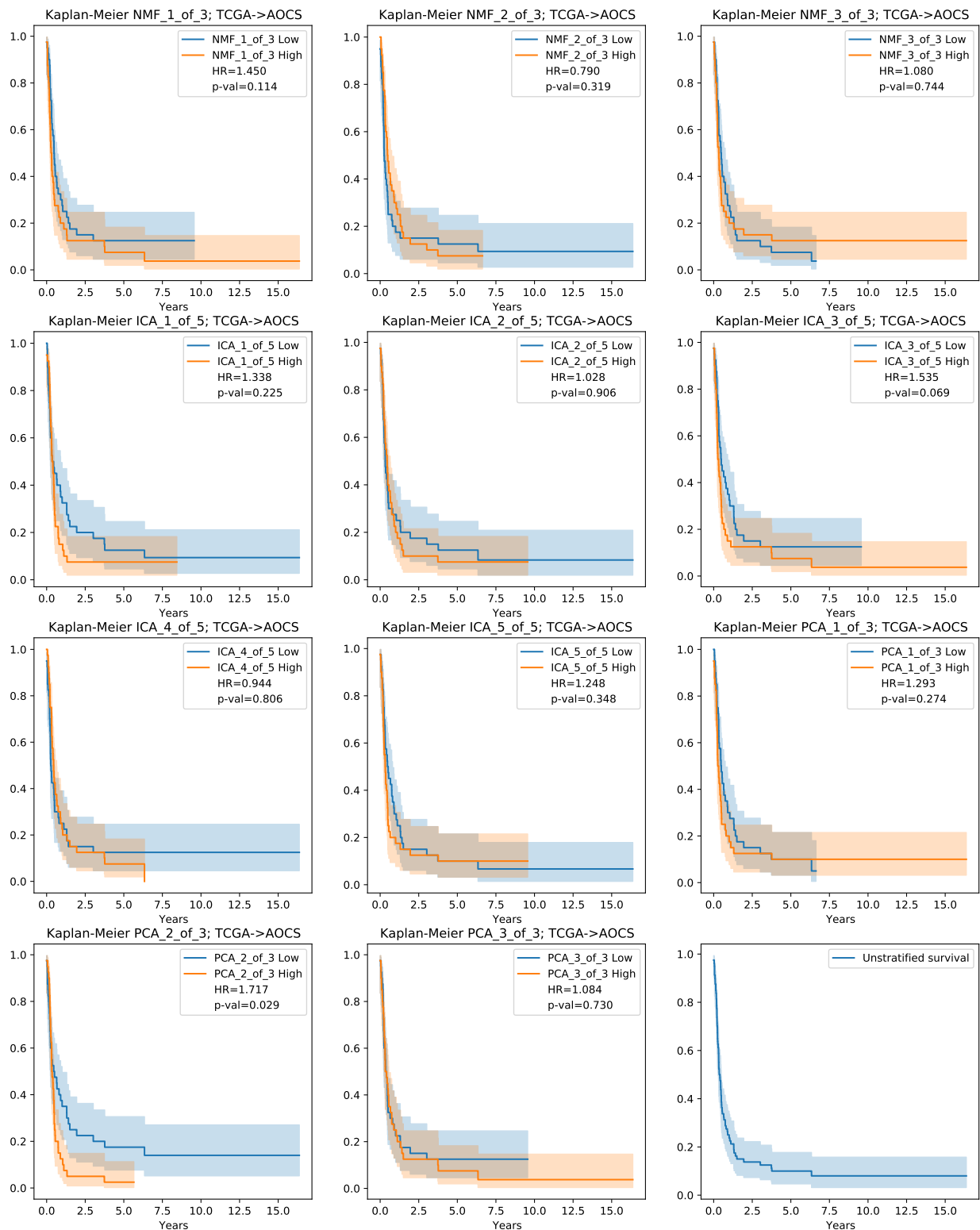


Figure 17: Kaplan-Meier plots for TCGA → TCGA for progression free survival (PFS).

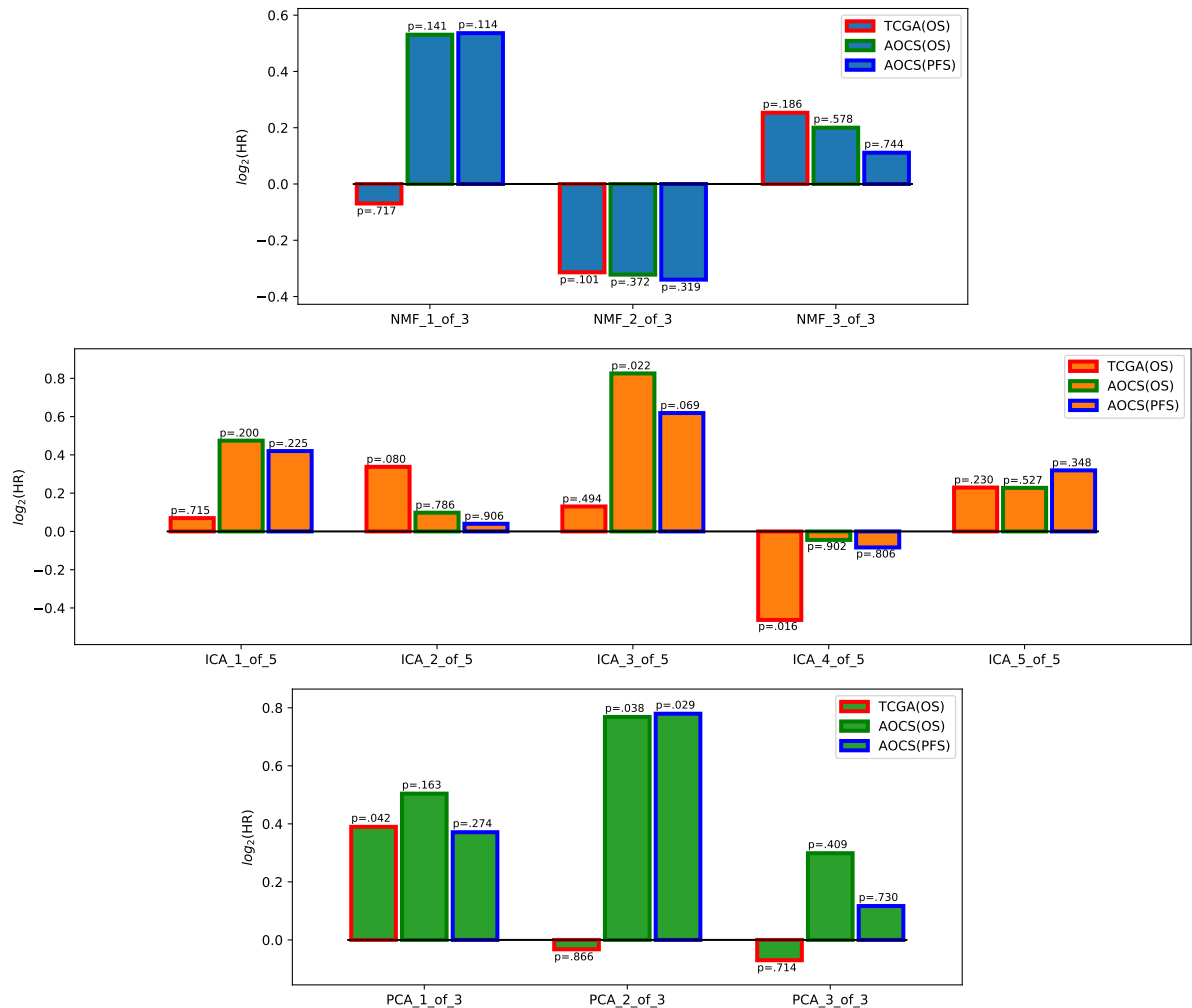


Figure 18: Visual summary of survival analysis as applied to TCGA(OS), AOCS(OS) and AOCS(PFS). Plots are divided by factorization method. Bar heights show $\log_2(\text{HR})$ with p-value also shown. For a component to have robust correlation with survival we expect all three of the analysis bars to pass a significance threshold *and* for the $\log_2(\text{HR})$ to be *in the same sense*. None achieve this.

WGD : Whole genome doubling – a marker of genome instability.

Cellularity : proportion of cells belonging to the tumour (as opposed to surrounding normal tissue).

HR Detect : A predictor of homologous repair deficiency based on established mutational features [16].

Mutational Load : A measure of the total number of mutations present in the tumour genome.

CNV Load : Copy-number variation, i.e. deviation from the normal diploid cell compliment.

The dendrogram clustering of metasamples (columns, top of figures) gives insights into the similarity of each metasample component, while the clustering of patients (rows, left of figures) offers insights into sub-populations of patients and how (in the case of AOCS only) these relate to metadata variables such as cellularity and mutational load. These topics will be taken up in the following discussion section.

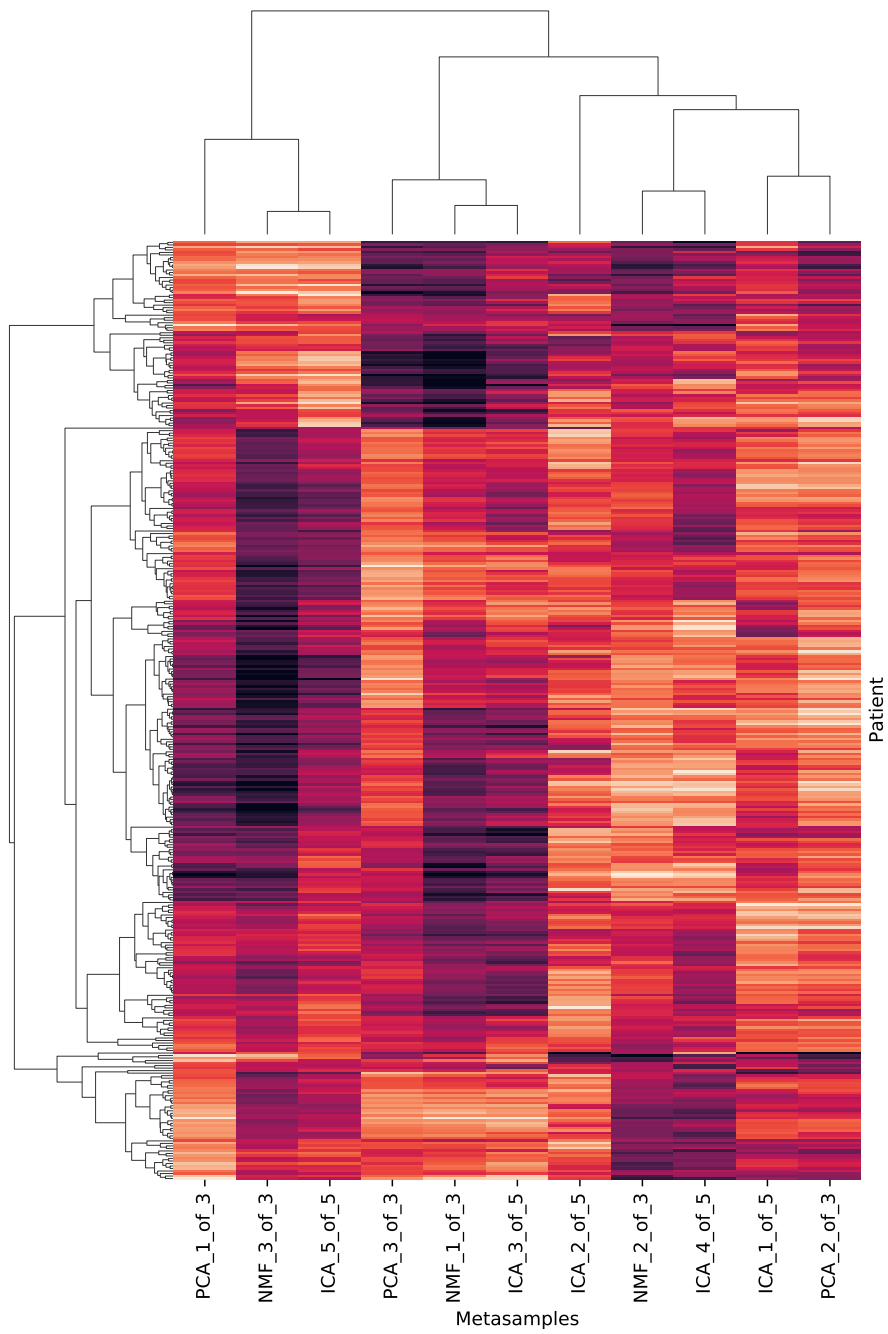


Figure 19: Heatmap of the metasamples matrix for the TCGA dataset, computed from metagenes factorized also TCGA. Clustering dendograms (based on a correlation distance) are shown between the metasamples (columns) and patients (rows).

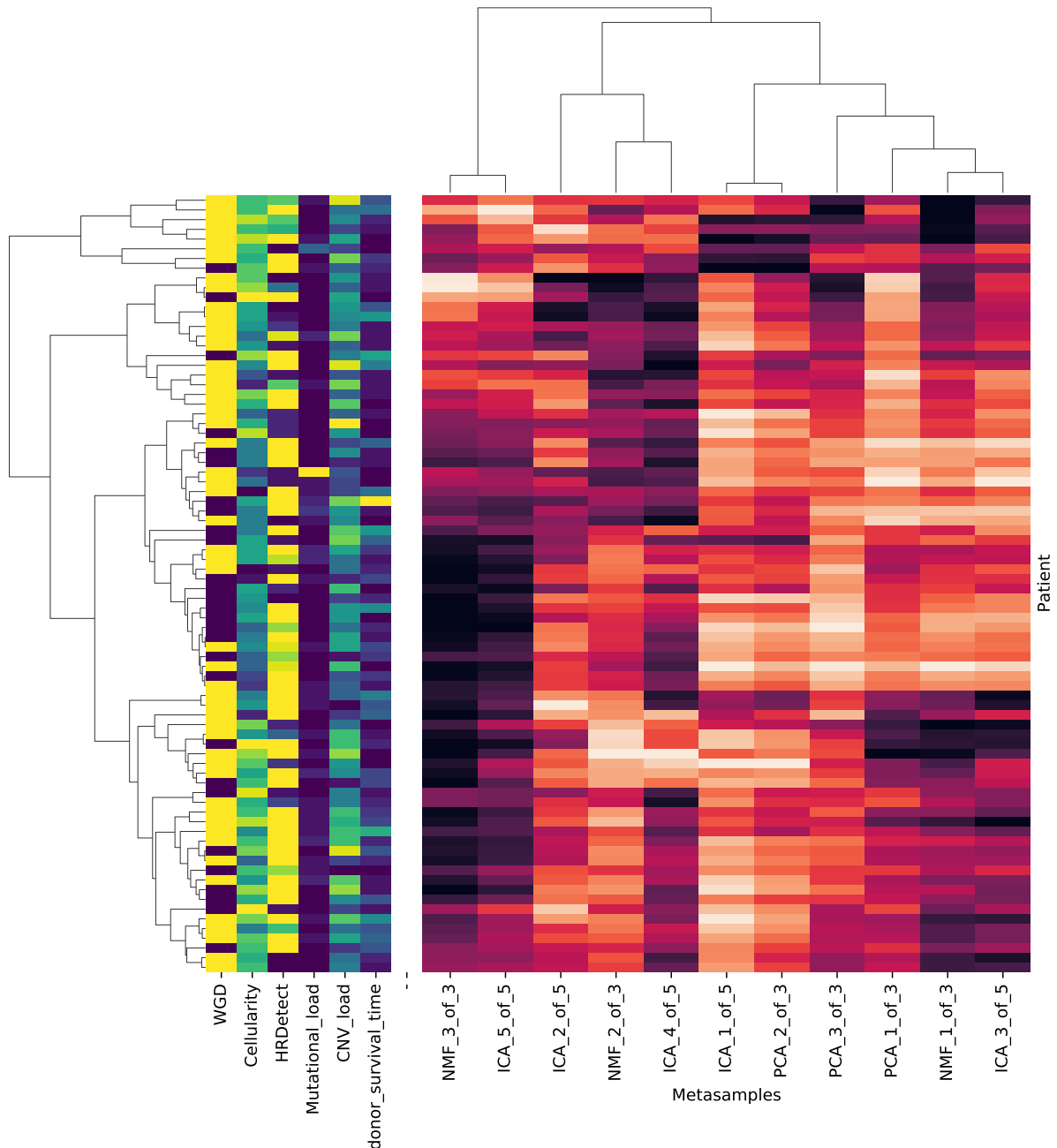


Figure 20: Heatmap of the metasamples matrix for the AOCS dataset, computed from metagenes factorized from the TCGA dataset. Several patient metadata variables are shown in columns to the left. (ToDo: key for metadata colouring).

4 Discussion

One valuable lesson from this work is the importance of accounting for sampling error, by bootstrapping, when considering the stability of factorizations and thence the selection of factorization rank. Several authors comment on the variability of NMF and ICA factorization due to algorithm initialisation [8, 5, 25], but most neglect sampling error which we have shown to be far more significant. Cantini *et al* [26] mention bootstrapping, in reference to the BIODICA package (for ICA factorization), but it is unclear whether this is applied to the input data to model sampling error. In the initial stages of the current work, BIODICA was used, and was found to recommend ranks of 14, 19 or 30. Yet we have seen that such high ranks on the small n=80 dataset leads to highly unstable factorizations when bootstrap modelling of sampling error is included.

These considerations lead to the selection of much lower ranks (fewer metagenes) than would otherwise be the case.

Considering the biological significance of each of the 11 extracted metagenes:

NMF 1-of-3 : this is related to the cellular structures and processes of the extra-cellular matrix (ECM), that is the proteins such as collagens which mediate the three-dimensional organisation of cells in a tissues. ECM molecular composition will vary substantially between tissue types, but is also known to play a part in many disease processes [27]. Thus, this metagene may simply reflect heterogeneity of tissues in the biopsied sample, or may have some deeper disease related significance.

NMF 2-of-3 : here we see enrichment of genes relating to the ribosomal subunit and the processes of RNA binding, implying perhaps a link with assembly of the ribosomal RNA-protein complex. Ribosomes are known to have a role in carcinogenesis, by dysregulation the RNA → protein translation, or mutations in ribosomal subunits impacting on cellular metabolism [28].

NMF 3-of-3 : no significant biological enrichment found.

ICA 1-of-5 and ICA 2-of-5 : no significant biological enrichment found.

ICA 3-of-5 : this component relates to processes of multicellular / extracellular organisation, and the ECM. It is therefore similar to NMF 1-of-3 above.

ICA 4-of-5 : this component is seen to relate to the ribosomal subunit (as NMF 2-of-3),

additionally membrane proteins in the respiratory complex, mitochondrial and the NADH dehydrogenase complex. Processes of organonitrogen biosynthesis are also highlighted.

ICA 5-of-5 : processes relating to regulation of immune response are enriched in this component, featuring genes from the major histocompatibility complex group, in particular the HLA- genes, allowing the immune system to recognise self from non-self. GO terms relating to the endoplasmic reticulum (ER) are also highlighted. It may be that this component is mainly sensitive to the immunohistochemical signature of patients, and therefore not of clinical interest.

PCA 1-of-3 : there is mention of ECM related terms, as for ICA 3-of-5 and NMF 1-of-3. However, there are also terms relating to the regulation of angiogenesis. It is known that tumours have a need for increased blood supply, and that expression level of factors promoting angiogenesis are associated with aggressiveness of tumour growth [29]. Two distinct subtypes of ovarian cancer have been identified, defined on the expression of angiogenesis related genes. Further, these subtypes have been found to inform clinical outcome [30]. Thus, this component might contain useful prognostic value.

PCA 2-of-3 : no significant biological enrichment found.

PCA 3-of-3 : this component has some similarity with ICA 5-of-5, in that it refers to regulation of immune processes (HLA- genes) and ER membrane. However, chemotaxis (cell movement) is also highlighted.

We have noted above that both NMF 1-of-3 and ICA 3-of-5 may be related to tissue type heterogeneity. We have also seen from metasample heatmap analysis that these two metagenes are associated with closely correlated metasamples in both the TCGA and OACS datasets, and also to have a moderately high Jaccard similarity of 0.39. Further, we observed that these components correlate negatively with cellularity. This is as one would expect: low cellularity implies a mixture of tumour and non-tumour cell types, resulting in variation of ECM composition.

Interestingly, the above summary of the gene enrichment results tentatively suggests component PCA 1-of-3 is most likely to have clinical prognostic value, based on a cursory look at the literature. This perhaps supports an earlier observation that, while not conclusive, component PCA-1-of-3 comes closest to demonstrating correlation with patient survival (section 2.9, figure 18).

How should we interpret those four components which demonstrate no significant enrichment with biological meaning? It is notable that all three methods have at least one such component.

Among these four, PCA 1-of-3 and ICA 1-of-5 have high (the highest) Jaccard similarity of 0.61. For all other pairs among these four Jaccard similarity is negligible. Perhaps these two components are picking up on similar technical variation between the samples?

4.1 Research questions revisited

TODO (sorry!).

4.2 Further work

This work has thrown up several possible lines of further study:

1. **Algorithm hyper-parameters.** NMF and ICA algorithms have a number of hyper-parameters, only a few of which were explored in this work. For example, NMF has parameters to encourage sparsity through L1 regularization. This should result in many (most?) metagene elements reducing to zero, and might offer a more robust means of selecting candidate genes to feed into gene enrichment analysis – replacing the current arbitrary 3 SD from the mean rule.
2. **Discovering batch effects.** It has been claimed (e.g. [2]) that matrix factorization methods are an effective means of identifying and removing batch effects. This could be explored by horizontally concatenating the TCGA and AOCS datasets (after gene set intersection), producing an $n = 80 + 274 = 354$ dataset with a substantial batch artefact. Factorizations of this combined dataset should be more robust because of the larger n . Does each of NMF, ICA and PCA naturally produce a component which correlates with batch?
3. **Selecting components from several factorization ranks.** In the current work, a single rank was selected for each method – 3, 5 an 3 for NMF, ICA and PCA respectively. Unlike PCA, components extracted by NMF and ICA do not ‘nest’ with rank; that is adding rank in general yields a new set of components. Thus one might, for NMF and ICA, perform factorizations at $k = 2, 3, 4, 5$, say, yielding $2 \times 15 = 30$ potential components in total. Jaccard similarity could be used to identify that subset of components which had the least overlap in detected genes. In this way, a larger number of components could be obtained without use of high factorization ranks which we have seen to be unstable.

4. **Cross-dataset factorization stability.** We went to considerable effort – through bootstrap sampling and cluster analysis – to select factorization ranks which we hoped would be robust and generalise well to other datasets. A way to confirm this robustness would be to perform the factorization / clustering pipeline on *both* datasets separately, yielding two sets of metagenes. In a perfect world, these metagenes would pair up identically (in-so-far as the two datasets had identical technical characteristics, drawn from identical population of patients). The Jaccard similarity heatmap could be used to verify this, and reject components which showed low cross-dataset similarity.
5. **Contrasting gene expression patterns between cancers.** The current work set out to find patterns of gene expression in HGSOC. Yet it is hard to say the highlighted patterns are specific to HGSOC, or generic to all cancers. One way of teasing out cancer specific patterns might be to take a similar approach to the previous item, but instead of looking for metagenes which are consistent between datasets, find those which are distinct. That said, there will likely be many more sophisticated approaches in the literature, given the clinical importance of the topic.
6. **Systematic comparison with published gene expression patterns.** In analysing the meaning of each metagene above, some tentative links were made with the research literature. But this was anecdotal and frankly not particularly scientific; searching on PubMed for GO terms associated with HGSOC and looking at one or two hits! A more systematic and ideally automated approach is required. The [Geo Profiles database](#) at NCBI, or the [Expression Atlas](#) at EMBL-BI might be possible starting points.

5 Conclusions

TODO

References

- [1] M. A. Lisio, L. Fu, A. Goyeneche, Z. H. Gao, and C. Telleria, “High-grade serous ovarian cancer: Basic sciences, clinical and therapeutic standpoints,” *International Journal of Molecular Sciences*, vol. 20, no. 4, 2019.

- [2] G. L. Stein-O'Brien, R. Arora, A. C. Culhane, A. V. Favorov, L. X. Garmire, C. S. Greene, L. A. Goff, Y. Li, A. Ngom, M. F. Ochs, Y. Xu, and E. J. Fertig, "Enter the Matrix: Factorization Uncovers Knowledge from Omics," oct 2018.
- [3] J. P. Brunet, P. Tamayo, T. R. Golub, and J. P. Mesirov, "Metagenes and molecular pattern discovery using matrix factorization," *Proceedings of the National Academy of Sciences of the United States of America*, vol. 101, no. 12, pp. 4164–4169, 2004.
- [4] P. Comon, "Independent component analysis, A new concept?," *Signal Processing*, vol. 36, no. 3, pp. 287–314, 1994.
- [5] N. Sompairac, E. Barillot, P. V. Nazarov, U. Czerwinska, L. Cantini, A. Biton, A. Molkenov, Z. Zhumadilov, F. Radvanyi, A. Gorban, U. Kairov, and A. Zinovyev, "Independent component analysis for unraveling the complexity of cancer omics datasets," *International Journal of Molecular Sciences*, vol. 20, no. 18, 2019.
- [6] L. Cantini, U. Kairov, A. De Reyniès, E. Barillot, F. Radvanyi, A. Zinovyev, and I. Birol, "Assessing reproducibility of matrix factorization methods in independent transcriptomes," *Bioinformatics*, vol. 35, no. 21, pp. 4307–4313, 2019.
- [7] G. Au-Yeung, P. M. Webb, A. Defazio, S. Fereday, M. Bressel, and L. Mileshkin, "Impact of obesity on chemotherapy dosing for women with advanced stage serous ovarian cancer in the Australian Ovarian Cancer Study (AOCS)," *Gynecologic Oncology*, vol. 133, no. 1, pp. 16–22, 2014.
- [8] U. Kairov, L. Cantini, A. Greco, A. Molkenov, U. Czerwinska, E. Barillot, and A. Zinovyev, "Determining the optimal number of independent components for reproducible transcriptomic data analysis," *BMC Genomics*, vol. 18, no. 1, pp. 1–13, 2017.
- [9] W. Kong, C. R. Vanderburg, H. Gunshin, J. T. Rogers, and X. Huang, "A review of independent component analysis application to microarray gene expression data.," *BioTechniques*, vol. 45, pp. 501–20, nov 2008.
- [10] S. I. Lee and S. Batzoglou, "Application of independent component analysis to microarrays," *Genome Biology*, vol. 4, no. 11, 2003.
- [11] C. Meng, O. A. Zelezniak, G. G. Thallinger, B. Kuster, A. M. Gholami, and A. C. Culhane, "Dimension reduction techniques for the integrative analysis of multi-omics data," *Briefings in Bioinformatics*, vol. 17, no. 4, pp. 628–641, 2016.

- [12] E. Barillot, L. Calzone, and P. Hupe, "Review of Computational Systems Biology of Cancer," *BioMedical Engineering OnLine*, vol. 12, no. 1, p. 76, 2013.
- [13] M. A. Cuello, S. Kato, and F. Liberona, "The impact on high-grade serous ovarian cancer of obesity and lipid metabolism-related gene expression patterns: the underestimated driving force affecting prognosis," *Journal of Cellular and Molecular Medicine*, vol. 22, no. 3, pp. 1805–1815, 2018.
- [14] C. Wang, S. M. Armasu, K. R. Kalli, M. J. Maurer, E. P. Heinzen, G. L. Keeney, W. A. Cliby, A. L. Oberg, S. H. Kaufmann, and E. L. Goode, "Pooled clustering of high-grade serous ovarian cancer gene expression leads to novel consensus subtypes associated with survival and surgical outcomes," *Clinical Cancer Research*, vol. 23, no. 15, pp. 4077–4085, 2017.
- [15] M. Pradhan, B. Risberg, C. G. Tropé, M. van de Rijn, C. B. Gilks, and C. H. Lee, "Gross genomic alterations and gene expression profiles of high-grade serous carcinoma of the ovary with and without BRCA1 inactivation," *BMC Cancer*, vol. 10, no. 1, pp. 1–8, 2010.
- [16] A. Ewing, A. Meynert, M. Churchman, G. R. Grimes, R. L. Hollis, C. S. Herrington, T. Rye, C. Bartos, I. Croy, M. Ferguson, T. McGoldrick, N. McPhail, N. Siddiqui, and S. Dowson, "Structural variants at the BRCA1/2 loci are a common source of homologous repair deficiency in high grade serous ovarian carcinoma," pp. 1–37, 2020.
- [17] B. Winterhoff, H. Hamidi, C. Wang, K. R. Kalli, B. L. Fridley, J. Dering, H.-W. Chen, W. A. Cliby, H.-J. Wang, S. Dowdy, B. S. Gostout, G. L. Keeney, E. L. Goode, and G. E. Konecny, "Molecular classification of high grade endometrioid and clear cell ovarian cancer using TCGA gene expression signatures," *Gynecologic oncology*, vol. 141, pp. 95–100, apr 2016.
- [18] A. M. Patch, E. L. Christie, D. Etemadmoghadam, D. W. Garsed, J. George, S. Fereday, K. Nones, P. Cowin, K. Alsop, P. J. Bailey, K. S. Kassahn, F. Newell, M. C. Quinn, S. Kazakoff, K. Quek, C. Wilhelm-Benartzi, E. Curry, H. S. Leong, A. Hamilton, L. Mileshkin, G. Au-Yeung, C. Kennedy, J. Hung, Y. E. Chiew, P. Harnett, M. Friedlander, M. Quinn, J. Pyman, S. Cordner, P. O'Brien, J. Leditschke, G. Young, K. Strachan, P. Waring, W. Azar, C. Mitchell, N. Traficante, J. Hendley, H. Thorne, M. Shackleton, D. K. Miller, G. M. Arnau, R. W. Tothill, T. P. Holloway, T. Semple, I. Harliwong, C. Nourse, E. Nourbakhsh, S. Manning, S. Idrisoglu, T. J. Bruxner, A. N. Christ, B. Poudel, O. Holmes, M. Anderson, C. Leonard, A. Lonie, N. Hall, S. Wood, D. F. Taylor, Q. Xu, J. Lynn Fink, N. Waddell, R. Drapkin, E. Stronach, H. Gabra, R. Brown, A. Jewell, S. H. Nagaraj, E. Markham, P. J. Wilson, J. Ellul, O. McNally, M. A. Doyle, R. Vedururu, C. Stewart, E. Lengyel, J. V. Pearson, N. Waddell, A. Defazio, S. M.

Grimmond, and D. D. Bowtell, “Whole-genome characterization of chemoresistant ovarian cancer,” *Nature*, vol. 521, pp. 489–494, may 2015.

- [19] A. W. Zhang, A. McPherson, K. Milne, D. R. Kroeger, P. T. Hamilton, A. Miranda, T. Funnell, N. Little, C. P. de Souza, S. Laan, S. LeDoux, D. R. Cochrane, J. L. Lim, W. Yang, A. Roth, M. A. Smith, J. Ho, K. Tse, T. Zeng, I. Shlafman, M. R. Mayo, R. Moore, H. Failmezger, A. Heindl, Y. K. Wang, A. Bashashati, D. S. Grewal, S. D. Brown, D. Lai, A. N. Wan, C. B. Nielsen, C. Huebner, B. Tessier-Cloutier, M. S. Anglesio, A. Bouchard-Côté, Y. Yuan, W. W. Wasserman, C. B. Gilks, A. N. Karnezis, S. Aparicio, J. N. McAlpine, D. G. Huntsman, R. A. Holt, B. H. Nelson, and S. P. Shah, “Interfaces of Malignant and Immunologic Clonal Dynamics in Ovarian Cancer,” *Cell*, vol. 173, no. 7, pp. 1755–1769.e22, 2018.
- [20] S. Kamble, A. Sen, R. Dhake, A. Joshi, D. Midha, and S. Bapat, “Clinical Stratification of High-Grade Ovarian Serous Carcinoma Using a Panel of Six Biomarkers,” *Journal of Clinical Medicine*, vol. 8, no. 3, p. 330, 2019.
- [21] F. Mairinger, A. Bankfalvi, K. W. Schmid, E. Mairinger, P. Mach, R. F. Walter, S. Borchert, S. Kasimir-Bauer, R. Kimmig, and P. Buderath, “Digital immune-related gene expression signatures in high-grade serous ovarian carcinoma: Developing prediction models for platinum response,” *Cancer Management and Research*, vol. 11, pp. 9571–9583, 2019.
- [22] A. Talhouk, J. George, C. Wang, T. Budden, T. Z. Tan, S. Derek, S. Kommoos, H. S. Leong, S. Chen, and M. P. Intermaggio, “Development and validation of the gene-expression Predictor of high-grade-serous Ovarian carcinoma molecular subTYPE (PrOTYPE),” 2020.
- [23] D. V. Klopfenstein, L. Zhang, B. S. Pedersen, F. Ramírez, A. W. Vesztrocy, A. Naldi, C. J. Mungall, J. M. Yunes, O. Botvinnik, M. Weigel, W. Dampier, C. Dessimoz, P. Flick, and H. Tang, “GOATOOLS: A Python library for Gene Ontology analyses,” *Scientific Reports*, vol. 8, no. 1, pp. 1–17, 2018.
- [24] C. Davidson-Pilon, J. Kalderstam, N. Jacobson, Sean-reed, B. Kuhn, P. Zivich, M. Williamson, AbdealiJK, D. Datta, A. Fiore-Gartland, A. Parij, D. WIllson, Gabriel, L. Moneda, K. Stark, A. Moncada-Torres, H. Gadgil, Jona, K. Singaravelan, L. Besson, M. S. Peña, S. Anton, A. Klintberg, J. Noorbakhsh, M. Begun, R. Kumar, S. Hussey, D. Golland, Jlim13, and A. Flaxman, “CamDavidsonPilon/lifelines: v0.24.16,” jul 2020.
- [25] G. Way and M. Zietz, *Sequential compression of gene expression across dimensionalities and methods reveals no single best method or dimensionality*. 2019.

- [26] L. Cantini, U. Kairov, A. De Reyniès, E. Barillot, F. Radvanyi, A. Zinovyev, and I. Birol, “SUPPLEMENTARY INFORMATION: Assessing reproducibility of matrix factorization methods in independent transcriptomes,” *Bioinformatics*, vol. 35, no. 21, pp. 4307–4313, 2019.
- [27] A. D. Theocharis, D. Manou, and N. K. Karamanos, “The extracellular matrix as a multitasking player in disease,” *FEBS Journal*, vol. 286, no. 15, pp. 2830–2869, 2019.
- [28] S. O. Sulima, I. J. F. Hofman, K. De Keersmaecker, and J. D. Dinman, “How Ribosomes Translate Cancer.,” *Cancer discovery*, vol. 7, no. 10, pp. 1069–1087, 2017.
- [29] N. Nishida, H. Yano, T. Nishida, T. Kamura, and M. Kojiro, “Angiogenesis in cancer,” *Vascular Health and Risk Management*, vol. 2, no. 3, pp. 213–219, 2006.
- [30] K. Glass, J. Quackenbush, D. Spentzos, B. Haibe-Kains, and G. C. Yuan, “A network model for angiogenesis in ovarian cancer,” *BMC Bioinformatics*, vol. 16, no. 1, pp. 1–17, 2015.

6 Appendices

6.1 Additional figures and plots

TODO - I'll likely move the AOCS survival plots here, and perhaps some of the GO lineages.

6.2 Gene enrichment raw results

TODO

6.3 Software libraries and versions

TODO